ogenic potential of OX could be attributed to its administration at lower dose levels (WHO 1991). In addition, OX exerted a tumor-promoting activity when administered to *N*-diethylnitrosamine (DEN)-treated rat livers at relatively high and repeated doses (Mitsumori et al. 1997). OX increased the number of hepatocellular foci positive for the placental form of glutathione *S*-transferase (GST-P), as a novel preneoplastic marker for chemical carcinogens (Kitahara et al. 1984), and decreased the levels of connexin 32, a protein responsible for gap junctional intercellular communication, which are considered to be a biological hallmark of tissues treated with tumor-promoting chemicals (Klaunig and Ruch 1990). Moreover, the same results were obtained in a two-stage carcinogenesis study of FEN in the livers of rats (Shoda et al. 1999). Considering that OX and FEN have no mutagenic activity in short-term genotoxicity assays (WHO 1991), these results suggest that OX exerts its tumor-promoting activity in the rat liver in a non-genotoxic or indirect genotoxic manner; however, its molecular mechanism has not yet been fully elucidated.

Oxidative stress has been recognised as an important factor involved in the pathogenesis of degenerative and inflammatory diseases, aging, and cancer (Wiseman and Halliwell 1996; Trush and Kensler 1991). Indeed, reactive oxygen species (ROS) are believed to play a pivotal role in the etiology of liver cancer, and ROS overproduction and subsequent oxidative DNA damage have been implicated in enhancing the development of hepatocellular tumors caused by agents such as the drug fenofibrate (Nishimura et al. 2007), the insecticide piperonyl butoxide (Muguruma et al. 2007) and p,p′-DDT (Harada et al. 2003). These compounds have been shown to increase gene expression levels of the transcription factor Nrf2-regulated genes such as glutathione peroxidise 2 (*Gpx2*), a NAD(P)H dehydrogenase (*Nqo1*), Glutathione *S*-transferase Yc2(*Yc2*), aflatoxin B1-aldehyde reductase (*Akr7a3*), and Glutathione *S*-transferase mu1(*Gstm1*). It is well known that Nrf2 binds to the antioxidant response element (ARE), a cis-acting sequence found in the 5′-flanking regions of these genes encoding a group of detoxification and antioxidant enzymes (McMahon et al. 2001), which are involved in protection against oxidative stress (Thimmulappa et al. 2002; Kwak et al. 2003). Glutathione peroxidase is the antioxidant enzyme that scavenges hydrogen peroxide and organic hydroperoxides, and thus protects cellular components against oxidative stress (Brigelius-Flohe 1999). Furthermore, Gpx2 may be involved in mammary carcinogenesis and cell proliferation in both rats and humans (Naiki-Ito et al. 2007). Nqo1 catalyses the obligatory two-electron reduction and detoxification of endogenous and environmental quinones (Riley and Workman 1992; Talalay et al. 1995). Yc2 catalyses the conjugation of glutathione to a variety of endogenous and xenobiotic electrophils (Hayes and Pulford 1995) and represents an important cellular defence by acting as scavengers of ROS (Hayes and McLellan 1999). Akr7a3 converts aflatoxin B1-dihydrodiol to the less toxic dialcohol metabolite and plays an important role in the detoxification of AFB1 by protecting against the formation of protein adducts (Hayes et al. 1993; Judah et al. 1993). *Gstm1* may play a protective role in defences against 4-hydroxynonenal- and hydrogen peroxide-induced oxidative stress in vitro (Raza et al. 2002) and both constitutive and oxidative stress-induced mRNA expression depends on the presence of Nrf2 in the liver (Chanas et al. 2002).

Recently, it has been suggested that repeated doses of the benzimidazole-derived anthelmintics albendazole and mebendazole induce lipid peroxidation and an imbalance of glutathione homeostasis in rat livers (Locatelli et al. 2004). These results imply the possible involvement of oxidative stress in OX- and FEN-induced rat hepatocarcinogenesis.

In the present study, the mechanism underlying the tumor-promoting ability of OX in the livers of rats was investigated with particular focus on gene expression and biochemical events affecting the cellular redox status. We have demonstrated that OX exhibits tumor-promoting activity that enhances oxidative stress and preneoplastic foci in a DEN-initiated hepatocarcinogenesis model in partially hepatectomized rats.

Materials and methods

Chemicals

Oxfendazole [methyl 5-(phenylsulfinyl)-2-benzimidazolecarbamate, OX; CAS No. 53716-50-0] and *N*-diethylnitrosamine [DEN; CAS No. 55-18-5] were purchased from Hayashi Pure Chemical Industries (Osaka, Japan) and Tokyo Kasei Kogyo (Tokyo, Japan) with purities of 99.7% and >99%, respectively.

Animals and experimental design

Animals received humane care in accordance with the Guide for Animal Experimentation by the Tokyo University of Agriculture and Technology. A total of 24 male F344/N rats aged 5 weeks were purchased from Japan SLC, Inc. (Shizuoka, Japan), maintained in an air-conditioned room with a 12-h light/dark cycle (room temperature, 24 ± 3°C; relative humidity, 55 ± 10%), and given free access to a powdered diet (Oriental MF; Oriental Yeast, Tokyo, Japan) and tap water. After a 1-week acclimatization period, a medium-term liver carcinogenesis bioassay (Ito et al. 2003) was performed by the following procedure. All animals received an intraperitoneal injection of DEN at a dose of 200 mg/kg body weight, and were fed a diet con-

taining 0% (basal diet) or 0.05% OX for 6 weeks starting 2 weeks after DEN initiation. All animals were subjected to two-thirds partial hepatectomy 1 week after OX treatment. Nine animals died after partial hepatectomy, while 15 animals survived (9 in the DEN alone group and 6 in the DEN + 0.05% OX group). Body weight and food consumption were measured once a week. At the end of the experiment, the rats were euthanized by exsanguination under ether anaesthesia, and the livers were excised and weighed; the sliced liver samples were fixed in 10% phosphate-buffered formalin for histopathology and immunohistochemistry. The remaining pieces of the livers were frozen in dry ice and stored at −80°C until further analysis.

Histopathology and immunohistochemistry

The fixed liver slices were dehydrated in graded ethanol, embedded in paraffin, sectioned, and stained with haematoxylin and eosin (H.E.) for histopathological examinations. Immunohistochemical staining of GST-P and proliferating cell nuclear antigen (PCNA) was performed by the following procedure. The deparaffinized liver sections were treated with 0.3% H_2O_2 in methanol for 30 min to block endogenous peroxidase and then incubated overnight at 4°C with rabbit anti-GST-P antibody (1:2,000 dilution; Medical and Biological Laboratories Co., Ltd., Aichi, Japan) or mouse anti-PCNA antibody (1:500 dilution; Dako, Glostrup, Denmark). For PCNA staining, the sections were heated by microwave in 10 mmol/l sodium citrate buffer (pH 6.0) before quenching the endogenous peroxidase activity. The avidin-biotin-peroxidase complex method (Vectastain Elite ABC system; Vector Laboratories, Burlingame, CA) was then employed with 3,3′-diaminobenzidine as a chromogen, followed by light counterstaining with haematoxylin.

The numbers and areas of GST-P-positive foci (>0.2-mm diameter) and the total areas of the liver sections were quantified using Scion Image (Scion Corp., Frederick, MD, USA). PCNA-positive nuclei were examined in a total of 20 fields (approximately 300–400 hepatocytes in each field) per animal, and the cells with positive nuclei (dark brown) were counted to determine the PCNA labelling index.

qRT-PCR analysis

The expression levels of the genes listed in Table 1 were quantified using quantitative real-time reverse transcription-polymerase chain reaction (qRT-PCR) analysis. The gene products are involved in the detoxification of xenobiotics and defences against oxidative stress responses (Dewa et al. 2007). Briefly, total RNA from five rats per treatment group was extracted using TRIzol reagent (Invitrogen Corp.), according to the manufacturer's instructions. The total RNA was reverse transcribed using ThermoScript reverse transcriptase (SuperScript III First-Strand Synthesis System; Invitrogen). All PCR reactions were performed using SYBR Green I chemistry (Applied Biosystems, CA, USA) and were carried out under the following conditions using an ABI PRISM 7000 Sequence Detection System (Applied Biosystems): incubation at 50°C for 2 min followed by 95°C for 10 min and 45 cycles of 95°C for 15 s and 60°C for 1 min. The forward and reverse primers listed in Table 1 were designed using the Primer Express 2.0 software following Applied Biosystems' instructions for optimal primer design. The relative differences in gene expression were calculated using cycle time (Ct) values that were first normalised to those of the hypoxanthine-guanine phosphoribosyltransferase (Hprt) gene, the endogenous control in the same sample, and then relative to a control Ct value by the 2-ddCt method (Livak and Schmittgen 2001). The data represent the average fold changes with standard deviation.

Table 1 Phase I and phase II enzyme/antioxidant genes examined in this study and their primer list

Accession no.	Gene description	Gene symbol	Forward	Reverse
X00469	Cytochrome P450, family 1, subfamily a, polypeptide 1	*Cypla1*	gccttcacatcagccacaga	ttgtgactctaaccacccagaatc
NM_012541	Cytochrome P450, family 1, subfamily a, polypeptide 2	*Cypla2*	aagcgccggttgcattg	tgcaggaggatggctaagaag
NM_183403	Glutathione peroxidase 2	*Gpx2*	accgalcccaagctcatca	tctcaaagttccaggacacatctg
NM_017000	NAD(P)H dehydrogenase, quinone 1	*Nqo1*	tccgccccaacttctg	tctgcgtgggccaataca
X78847	Glutathione S-transferase Yc2 subunit	*Yc2*	aagctgagcagggctgatgt	acaatgcctgggtccatctc
NM_013215	Aldo-keto reductase family 7, member A3 (aflatoxin aldehyde reductase)	*Akr7a3*	ccgctttcttgggaatccat	ggcgatgccattgaagtgt
NM_020540	Glutathione S-transferase, mu 1	*Gstm1*	gaacgttcgcggacttactca	acgtatctcttctcctcatagtttgaatct
NM_012600	Malic enzyme 1	*Me1*	cgaccagcaaagctgagtgtt	ctgccgctggcaaagatc
NM_012583	Hypoxanthine guanine phosphoribosyl transferase[a]	*Hprt*	gccgaccggttctgtcat	tcataacctggttcatcatcactaatc

[a] Control gene for normalization of relative gene expression

Preparation of microsomal fraction

The microsomal fractions were obtained according to the method of Yoshihara et al. (2001). Briefly, the liver samples from each treatment group were homogenised with three volumes of ice-cold 0.25 mol/l sucrose −0.05 mol/l Tris-HCl buffer (pH 7.4) using a glass-Teflon homogeniser. The homogenate was centrifuged at 700*g* for 10 min, and the supernatant was centrifuged at 10,000 *g* for 20 min. The resultant supernatant was further centrifuged at 105,000 *g* for 60 min, and the resultant pellet was resuspended and centrifuged again at 105,000*g* for 60 min. Finally, the pellet was resuspended in the 0.25 mol/l sucrose−0.05 mol/l Tris-HCl buffer (pH 7.4) as the microsomal fraction and stored at −80°C. The microsomal protein concentrations were determined by a BCA Protein Assay Kit (Pierce, IL, USA).

Microsomal reactive oxygen species production

NADPH-dependent microsomal ROS production was determined by measuring the oxidation of 2′,7′-dichlorodihydrofluorescein diacetate (H_2DCFDA) to its fluorescent product 2′, 7′-dichlorofluorescein (DCF) in liver microsomes according to the method of Schlezinger et al. (1999). Briefly, 0.1 mg of microsomal protein was incubated with 5 μmol/l H_2DCFDA (Invitrogen) in Hank's balanced salt solution (Invitrogen) at 30°C for 15 min. After incubation, this microsomal solution was transferred into a 96-well plate. The reactions were initiated with 1.4 mmol/l NADPH (Wako Pure Chemical Industries), and the fluorescence was monitored over 5 min using the Synergy HT Multi-Detection Microplate Reader (BioTek, VT, USA) with excitation and emission wavelengths of 485 and 528 nm, respectively. In some cases, SKF-525A (Toronto Research Chemicals, ON, Canada), a well-known inhibitor of cytochrome P450, was added to the well at a final concentration of 0.1 mmol/l. DCF production (pmol min^{-1} mg $protein^{-1}$) was obtained from standard curves prepared using DCF.

Western blotting

A total of 20 μg of microsomal proteins was electrophoresed on a 10% sodium dodecyl sulphate (SDS) gel, transferred to a polyvinylidene difluoride (PVDF) membrane (Hybond-P; GE Healthcare), and blocked. The membrane was incubated with anti-CYP1A1 (1:400 dilution; Santa Cruz Biotechnology, CA, USA) or anti-CYP2E1 (1:1,000 dilution; Biomol International, PA, USA) overnight at 4°C, followed by incubation in goat anti-rabbit IgG (horseradish peroxidase (HRP)-conjugated, 1:10,000 dilution; GE Healthcare) for 2 h at room temperature. The immunoproducts were visualised using ECL Plus™ Western blotting detection reagents (GE Healthcare).

Determination of 8-OHdG and TBARS levels

Oxidative DNA damage and lipid peroxidation in the livers were estimated on the basis of the levels of 8-hydroxydeoxyguanosine (8-OHdG) and thiobarbituric acid-reactive substances (TBARS), respectively.

The 8-OHdG levels in liver DNA were determined using the method of Umemura et al. (2006). Briefly, nuclear DNA was isolated from 0.3 g of a wet weight sample using a DNA Extractor WB Kit (Wako Pure Chemical Industries) containing an antioxidant NaI solution to dissolve the cellular components. For further prevention of autooxidation in the cell-lysis step, deferoxamine mesylate was added to the lysis buffer (Helbock et al. 1998). The DNA was digested into deoxynucleotides with nuclease P1 and alkaline phosphatase. The levels of 8-OHdG (8-OHdG/10^5 deoxyguanosine) were then assessed by high-performance liquid chromatography with an electrochemical detection system (Coulochem II; ESA Biosciences, Inc., MA, USA) according to the running condition previously reported (Umemura et al. 2006).

The levels of hepatic TBARS were determined using the method of Ohkawa et al. (1979). Briefly, 0.2 ml of liver homogenate in 1.15% KCl, 0.2 ml of 8.1% SDS and 3.0 ml of 0.4% thiobarbituric acid in 10% acetic acid (pH 3.5) were mixed, heated at 95°C for 60 min and then cooled. The reaction mixture was centrifuged at 4,000 rpm for 10 min after adding 1.0 ml of distilled water and 5.0 ml of *n*-butanol and pyridine (15:1 v/v). The absorbance of the resulting solution was determined spectrophotometrically at 532 nm using a Synergy HT Multi-Detection Microplate Reader (BioTek). The levels of TBARS were expressed as the equivalents of malondialdehyde (MDA) amounts that were produced from 1,1,3,3-tetramethoxypropane.

Statistical analysis

All data are expressed as means with their standard deviations. The statistical significance of differences between the control and the OX-treated group was determined by the Student's *t* test or the Aspin-Welch's *t* test. A *p* value of less than 0.05 was regarded as statistically significant.

Results

Body and liver weights, and histopathological findings

Throughout the experimental period, OX treatment affected neither clinical symptoms nor food consumption. Body weight gains in OX-treated rats were suppressed from 2 to 3 weeks after partial hepatectomy; however the final body weight was not changed compared with that of animals in

the DEN alone group (data not shown). The absolute and relative liver weights were significantly increased in OX-treated rats compared with rats in the DEN alone group (Table 2). Histopathologically, OX induced hepatocellular hypertrophy and vacuolation of hepatocytes, which were the earliest signs of a compound-related effect in rats.

Table 2 Changes in parameters for body weight, liver weight, GST-P positive foci, oxidative damage and cell proliferation

Group	DEN + Basal diet	DEN + 0.05% OX
No. of rats examined	9	6
Final body weight (g)	253.3 ± 13.4	255.1 ± 14.4
Absolute liver weight (g)	6.2 ± 0.5	8.3 ± 0.6**
Relative liver weight (g/100 g body weight)	2.4 ± 0.1	33. ± 0.1**
GST-P positive foci (≥0.2 mm)		
Numbers (number/cm^2)	4.02 ± 1.94	12.74 ± 5.66*
Ares (mm^2/cm^2)	0.11 ± 0.07	0.21 ± 0.10*
8-OHdG (8-OHdG/10^5 dG)	0.16 ± 0.01	0.20 ± 0.02*
TBARS (nmol MDA/mg protein)	0.95 ± 0.06	1.14 ± 0.09*
PCNA-positive cells (%)	1.42 ± 0.32	4.18 ± 1.04**

Each quantitative data represents mean ± SD

*,** Significantly different from DEN control ($p < 0.05$, 0.01, respectively, Aspin–Welch's t test)

Effects of OX treatment on GST-P-positive foci and cell proliferation

The numbers and areas of GST-P-positive foci in the OX-treated group were significantly increased compared with those in the DEN alone group (Table 2). In addition, the effect of OX on cell proliferation was evaluated by immunohistochemistry for PCNA (Table 2). The number of PCNA-positive hepatocytes was significantly increased in OX-treated animals ($p < 0.01$).

Increased expression of genes encoding phase I and phase II drug-metabolizing enzymes

In order to evaluate the effect of OX on the hepatic expression of xenobiotic detoxification- and oxidative stress-related genes, qRT-PCR analysis was performed in the livers of five rats per group using the primers listed in Table 1. Significant increases in the expression levels of genes encoding phase I drug-metabolizing enzymes, such as *Cyp1a1*, *Cyp1a2* and *Nqo1*, were observed in animals in the OX-treated group (Fig. 1). OX also significantly induced the expression of NF-E2-related factor 2 (Nrf2)-regulated genes, such as *Gpx2*, *Yc2*, *Afar*, *Gstm1*, *Me1* (and also *Nqo1*), the products of which mainly functioned as phase II drug-metabolizing enzymes (Fig. 1).

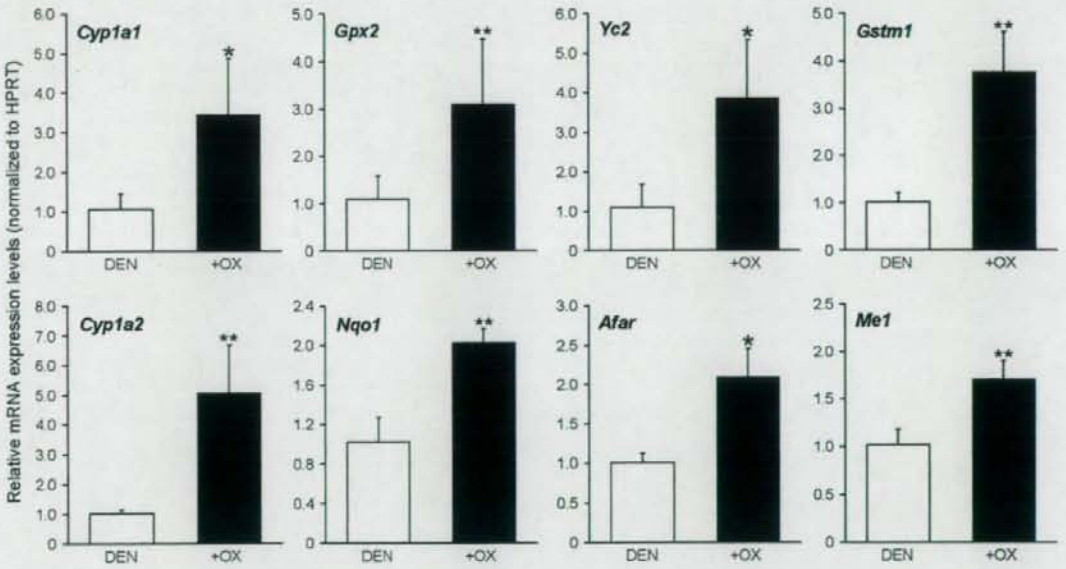

Fig. 1 Increased mRNA expression levels of phase I and phase II drug-metabolizing enzymes, and Nrf2-regulated molecules confirmed by quantitative real-time RT-PCR (qRT-PCR). Each column represents the mean + SD of the increased mRNA expression levels in the livers of 5 partially hepatectomized rats given 0% (*white column*) or 0.05% (*black column*) of OX after DEN initiation. *, ** indicates significant differences from DEN control ($p < 0.05$, 0.01 respectively; Aspin–Welch's t test)

Enhancement of microsomal ROS production

In order to estimate the cellular sources of ROS, NADPH-dependent ROS production was measured in isolated liver microsomes (Fig. 2a). Without NADPH, oxidised H_2DCFDA was not observed as an indicator of ROS production. However, ROS production was drastically enhanced by the addition of NADPH into the microsomal system, and its amount was statistically increased in rats given 0.05% OX compared with those in the DEN alone group. A well-known inhibitor of P450—SKF-525A—effectively inhibited these enhancements. Furthermore, the protein expression of CYP1A1 was concomitantly increased in microsomes isolated from the livers of rats treated with OX. On the other hand, the protein expression of CYP2E1, which was reported to predominantly generate ROS and to be related to oxidative stress (Gonzalez 2005), was unchanged by OX treatment (Fig. 2b).

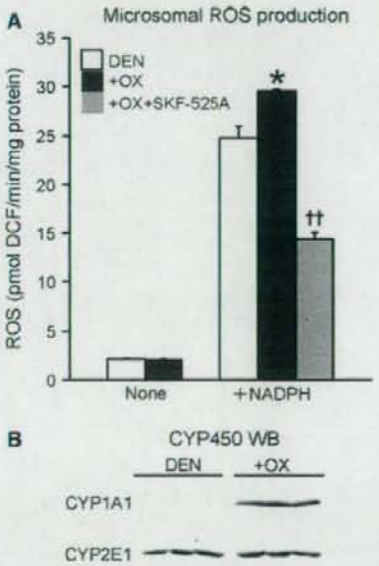

Fig. 2 Enhancement of ROS production and CYP1A1 protein expression in hepatic microsomes isolated from rats given OX. **a** NADPH-dependent microsomal ROS production was measured using the fluorescent probe H_2DCFDA. Each column represents the mean + SD values of ROS production in isolated microsomes from the livers of 9 or 6 partially hepatectomized rats given 0% (*white column*) or 0.05% of OX (*black column*) after DEN initiation. The *gray column* shows that the in vitro addition of SKF-525A (0.1 mmol/l) significantly suppresses ROS production in microsomes isolated from rats treated with 0.05% OX. *indicates significant differences from DEN control ($p < 0.05$; Aspin–Welch's t test). †† indicates significant suppression of ROS production by SKF-525A in rats treated with 0.01% OX ($p < 0.01$; Aspin-Welch's t test). **b** Western blot analysis for CYP1A1 and CYP2E1 protein expression for each microsome fraction used in (**a**)

Increase in oxidative stress changes

In order to evaluate whether oxidative damage to cellular components occurs during the formation of preneoplastic foci, 8-OHdG content and the level of TBARS formation were determined in livers (Table 2). The contents of 8-OHdG and TBARS were slightly but significantly increased in rats given 0.05% OX compared with those in the DEN alone group.

Discussion

OX, FEN, and their prodrug febantel (FB) have been widely utilized as anthelmintics in veterinary fields. FEN is metabolically interconvertible to OX, which is its most effective pharmacological form. FB is not a benzimidazole, but is converted in vivo by cyclization to FEN and subsequent oxidation at the sulphur atom to OX; thus, both FEN and FB are metabolized to OX. These three anthelmintics showed no apparent mutagenicity in numerous tests, including the Ames/Salmonella test, in vivo cytogenetics assays, and micronucleus assays (WHO 1991). With regard to their carcinogenicity, the 50th meeting of JECFA finally concluded that OX has no carcinogenic potential in rats and mice although OX might have tumor-promoting potential in rats; thus, the acceptable daily intake (ADI) of 0–7 μg/kg/day was set as a group ADI for OX, FEN and FB in JECFA (WHO 1999). However, the mechanisms underlying the tumor-promotion activity of OX in rats, at the molecular level, have still not been clarified.

Quantitative real-time PCR analysis revealed that phase I (*Cyp1a1*, *Cyp1a2*) drug-metabolizing enzymes were up-regulated in the livers of rats treated with OX. The induction of *Cyp1a1* and *Cyp1a2* observed in this study was in agreement with previous reports on several benzimidazole class compounds. OX induced CYP1A2 protein in the rabbit liver (Gleizes et al. 1991); FEN, albendazole and mebendazole induced CYP1A1 and CYP1A2 proteins in primary rat hepatocytes and HepG2 cells (Baliharova et al. 2003); thiabendazole, an anthelmintic and fungicide, induced *Cyp1a1* in rabbit hepatocytes in in vitro conditions (Aix et al. 1994); omeprazole, a gastric pump inhibitor, induced *Cyp1a1* and *Cyp1a2* in primary human hepatocytes (Diaz et al. 1990) and rat hepatocytes (Lemaire et al. 2004). The activation of *Cyp1a1* gene expression induced by omeprazole and thiabendazole does not require their binding to the aryl hydrocarbon receptor (Daujat et al. 1992; Aix et al. 1994), but it depends on a protein tyrosine kinase-mediated signal transduction pathway in HepG2 cells (Kikuchi et al. 1998) and rat hepatocytes (Lemaire et al. 2004). Indeed, benzimidazoles are atypical CYP1A inducers, which do not require their binding to AhR to induce CYP1A enzymes.

It has been reported that CYP1A1 induction is also related to the production of reactive oxygen species (ROS) induced not only by classical AhR ligands, such as TCDD (Park et al. 1996; Knerr et al. 2006) and coplanar polychlorinated biphenyl congeners (Schlezinger et al. 2006), but also the atypical, non-AhR ligand dicyclanil, which is an insecticide (Moto et al. 2005). Indeed, we have confirmed that microsomes isolated from the livers of rats treated with OX showed enhanced ROS production with a concomitant increase in CYP1A1 protein expression. It is generally accepted that microsomal CYP450s sequentially transfer 2 electrons to oxygen from microsomal NADPH-cytochrome P450 reductase with the subsequent formation of an oxygenated substrate and water (Poulos and Raag 1992). Although electron transfer is normally a well-coupled process, superoxide and H_2O_2 may be released in the presence of CYP1A inducers that are poorly metabolised. Indeed, PCB increases CYP1A1-dependent microsomal ROS production in the livers of rats as well as scup (*Stenotomus chrysops*) (Schlezinger et al. 2006). Therefore, excessive amounts of OX can induce CYP1A enzymes and subsequently enhance microsomal ROS production. On the other hand, Shertzer et al. (2006) recently reported that TCDD decreased hepatic ATP levels and altered the mitochondrial integrity in mice, which contributed to generate an oxidative stress such as oxidative DNA damages. In the present study, we have not examined the effect of OX treatment on mitochondrial functions, and therefore it is necessary to perform further studies with regard to its tumor modifying effect as a future work.

In addition, we observed increased gene expression levels of Nrf2-regulated, anti-oxidative stress genes (*Gpx2*, *Nqo1*, *Yc2*, *Akr7a3*, *Gstm1* and *Me1*) by quantitative real-time RT-PCR. In these genes, Me1 is a NAD(P)H-regenerating enzyme, and its increased expression may be beneficial for the function of the detoxifying enzymes, directly (NQO1, Akr7a3), or indirectly (Gpx2, Yc2) (Thimmulappa et al. 2002). Collectively, these results suggest that OX triggers oxidative stress responses, and that the gene expression levels of phase I and phase II enzymes are intrinsically induced to maintain the cellular redox balance.

We also estimated whether resultant oxidative damage occurs in the cellular components during preneoplastic foci formation. The amount of 8-OHdG in the nuclear DNA of rats given OX was significantly higher than that in the nuclear DNA of rats in the DEN alone group. 8-OHdG adducts have been reported to cause misreading of the DNA sequence during replication, thereby inducing G:C to T:A transversion, which is involved in carcinogenesis (Cheng et al. 1992). In fact, some CYP1A inducers such as dicyclanil and piperonyl butoxide increase the hepatic 8-OHdG levels during their hepatocarcinogenesis in mice or rats (Moto et al. 2005; Muguruma et al. 2007), and therefore, it is speculated that increases of 8-OHdG attributed to OX treatment may contribute its hepatocellular tumor promoting activity. In addition, OX induced a slight but significant increase in the level of lipid peroxidation. A positive correlation between lipid peroxidation and the induction of preneoplastic lesions has been reported in the livers of rats treated with DEN followed by treatment with 2-acetylaminofluorene and partial hepatectomy (Sanchez-Perez et al. 2005). In addition, the cellular level of lipid peroxidation paralleled the degree of malignancy in a comparison between a baby hamster kidney cell line (BHK-21/C13) and its polyoma virus-transformed malignant counterpart (Goldring et al. 1993). Our data suggest that OX induces sustained oxidative stress in the livers of rats, which accounts for, at least in part, the enhancement in microsomal ROS production and an increased level of oxidative DNA damage as well as lipid peroxidation. Such oxidative stress responses overwhelming detoxifying systems might contribute to the tumor-promoting activity of OX.

In conclusion, we have demonstrated that OX exhibits tumor-promoting activity that enhances oxidative stress and preneoplastic foci in a DEN-initiated hepatocarcinogenesis model in partially hepatectomized rats. The prolongation of this tumor-promotion effect may induce hepatocellular tumors in rats if high doses of OX are administered for a long term.

Acknowledgments This research was partly supported by a grant-in-aid for research on the safety of veterinary drug residues in food of animal origin from the Ministry of Health, Labor and Welfare of Japan (H19-shokuhin-ippan-011).

References

Aix L, Rey-Grobellet X, Larrieu G, Lesca P, Galtier P (1994) Thiabendazole is an inducer of cytochrome P4501A1 in cultured rabbit hepatocytes. Biochem Biophys Res Commun 202:1483–1489

Baliharova V, Skalova L, Maas RF, De Vrieze G, Bull S, Fink-Gremmels J (2003) The effects of benzimidazole anthelmintics on P4501A in rat hepatocytes and HepG2 cells. Res Vet Sci 75:61–69

Brigelius-Flohe R (1999) Tissue-specific functions of individual glutathione peroxidases. Free Radic Biol Med 27:951–965

Chanas SA, Jiang Q, McMahon M, McWalter GK, McLellan LI, Elcombe CR, Henderson CJ, Wolf CR, Moffat GJ, Itoh K, Yamamoto M, Hayes JD (2002) Loss of the Nrf2 transcription factor causes a marked reduction in constitutive and inducible expression of the glutathione S-transferase Gsta1, Gsta2, Gstm1, Gstm2, Gstm3 and Gstm4 genes in the livers of male and female mice. Biochem J 365:405–416

Cheng KC, Cahill DS, Kasai H, Nishimura S, Loeb LA (1992) 8-Hydroxyguanine, an abundant form of oxidative DNA damage, causes G—T and A—C substitutions. J Biol Chem 267:166–172

Daujat M, Peryt B, Lesca P, Fourtanier G, Domergue J, Maurel P (1992) Omeprazole, an inducer of human CYP1A1 and 1A2, is not a ligand for the Ah receptor. Biochem Biophys Res Commun 188:820–825

Delatour P, Parish R (1986) Benzimidazole anthelmintics and related compounds: toxicity and evaluation of residues. In: Rico AG (ed) Drug residues in animals. Academic Press, New York, pp 175–204

Dewa Y, Nishimura J, Muguruma M, Matsumoto S, Takahashi M, Jin M, Mitsumori K (2007) Gene expression analyses of the liver in rats treated with oxfendazole. Arch Toxicol 81:647–654

Diaz D, Fabre I, Daujat M, Saint Aubert B, Bories P, Michel H, Maurel P (1990) Omeprazole is an aryl hydrocarbon-like inducer of human hepatic cytochrome P450. Gastroenterology 99:737–747

Gleizes C, Eeckhoutte C, Pineau T, Alvinerie M, Galtier P (1991) Inducing effect of oxfendazole on cytochrome P450IA2 in rabbit liver. Consequences on cytochrome P450 dependent monooxygenases. Biochem Pharmacol 41:1813–1820

Goldring CE, Rice-Evans CA, Burdon RH, Rao R, Haq I, Diplock AT (1993) Alpha-Tocopherol uptake and its influence on cell proliferation and lipid peroxidation in transformed and nontransformed baby hamster kidney cells. Arch Biochem Biophys 303:429–435

Gonzalez FJ (2005) Role of cytochromes P450 in chemical toxicity and oxidative stress: studies with CYP2E1. Mutat Res 569:101–110

Harada T, Yamaguchi S, Ohtsuka R, Takeda M, Fujisawa H, Yoshida T, Enomoto A, Chiba Y, Fukumori J, Kojima S, Tomiyama N, Saka M, Ozaki M, Maita K (2003) Mechanisms of promotion and progression of preneoplastic lesions in hepatocarcinogenesis by DDT in F344 rats. Toxicol Pathol 31:87–98

Hayes JD, Judah DJ, Neal GE (1993) Resistance to aflatoxin B1 is associated with the expression of a novel aldo-keto reductase which has catalytic activity towards a cytotoxic aldehyde-containing metabolite of the toxin. Cancer Res 53:3887–3894

Hayes JD, McLellan LI (1999) Glutathione and glutathione-dependent enzymes represent a co-ordinately regulated defence against oxidative stress. Free Radic Res 31:273–300

Hayes JD, Pulford DJ (1995) The glutathione S-transferase supergene family: regulation of GST and the contribution of the isoenzymes to cancer chemoprotection and drug resistance. Crit Rev Biochem Mol Biol 30:445–600

Helbock HJ, Beckman KB, Shigenaga MK, Walter PB, Woodall AA, Yeo HC, Ames BN (1998) DNA oxidation matters: The HPLC-electrochmical detection assay of 8-oxo-deoxyguanosine and 8-oxo-deoxyguanine. Proc Natl Acad Sci USA 95:288–293

Ito N, Tamano S, Shirai T (2003) A medium-term rat liver bioassay for rapid in vivo detection of carcinogenic potential of chemicals. Cancer Sci 94:3–8

Jacobs DEJ, Taylor MA (2001) Drugs used in the treatment and control of parasitic infections. In: Bishop J (ed) The veterinary formulary, 5th edn edn. Pharmaceutical Press, London, pp 219–245

Judah DJ, Hayes JD, Yang JC, Lian LY, Roberts GC, Farmer PB, Lamb JH, Neal GE (1993) A novel aldehyde reductase with activity towards a metabolite of aflatoxin B1 is expressed in rat liver during carcinogenesis and following the administration of an antioxidant. Biochem J 292:13–18

Kikuchi H, Hossain A, Yoshida H, Kobayashi S (1998) Induction of cytochrome P-450 1A1 by omeprazole in human HepG2 cells is protein tyrosine kinase-dependent and is not inhibited by alpha-naphthoflavone. Arch Biochem Biophys 358:351–358

Kitahara A, Satoh K, Nishimura K, Ishikawa T, Ruike K, Sato K, Tsuda H, Ito N (1984) Changes in molecular forms of rat hepatic glutathione S-transferase during chemical hepatocarcinogenesis. Cancer Res 44:2698–2703

Klaunig JE, Ruch RJ (1990) Role of inhibition of intercellular communication in carcinogenesis. Lab Invest 62:135–146

Knerr S, Schaefer J, Both S, Mally A, Dekant W, Schrenk D (2006) 2, 3, 7, 8-Tetrachlorodibenzo-p-dioxin induced cytochrome P450s alter the formation of reactive oxygen species in liver cells. Mol Nutr Food Res 50:378–384

Kwak MK, Wakabayashi N, Itoh K, Motohashi H, Yamamoto M, Kensler TW (2003) Modulation of gene expression by cancer chemopreventive dithiolethiones through the Keap1-Nrf2 pathway. Identification of novel gene clusters for cell survival. J Biol Chem 278:8135–8145

Lemaire G, Delescluse C, Pralavorio M, Ledirac N, Lesca P, Rahmani R (2004) The role of protein tyrosine kinases in CYP1A1 induction by omeprazole and thiabendazole in rat hepatocytes. Life Sci 74:2265–2278

Livak KJ, Schmittgen TD (2001) Analysis of relative gene expression data using real-time quantitative PCR and the 2 (−Delta Delta C(T)) method. Methods 25:402–408

Locatelli C, Pedrosa RC, De Bem AF, Creczynski-Pasa TB, Cordova CA, Wilhelm-Filho D (2004) A comparative study of albendazole and mebendazole-induced, time-dependent oxidative stress. Redox Rep 9:89–95

McMahon M, Itoh K, Yamamoto M, Chanas SA, Henderson CJ, McLellan LI, Wolf CR, Cavin C, Hayes JD (2001) The Cap'n'Collar basic leucine zipper transcription factor Nrf2 (NF-E2 p45-related factor 2) controls both constitutive and inducible expression of intestinal detoxification and glutathione biosynthetic enzymes. Cancer Res 61:3299–3307

Mitsumori K, Onodera H, Shoda T, Uneyama C, Imazawa T, Takegawa K, Yasuhara K, Watanabe T, Takahashi M (1997) Liver tumour-promoting effects of oxfendazole in rats. Food Chem Toxicol 35:799–806

Moto M, Okamura M, Muto T, Kashida Y, Machida N, Mistumori K (2005) Molecular pathological analysis on the mechanism of liver carcinogenesis in dicyclanil-treated mice. Toxicology 207:419–436

Muguruma M, Unami A, Kanki M, Kuroiwa Y, Nishimura J, Dewa Y, Umemura T, Oishi Y, Mitsumori K (2007) Possible involvement of oxidative stress in piperonyl butoxide induced hepatocarcinogenesis in rats. Toxicology 236:61–75

Naiki-Ito A, Asamoto M, Hokaiwado N, Takahashi S, Yamashita H, Tsuda H, Ogawa K, Shirai T (2007) Gpx2 is an overexpressed gene in rat breast cancers induced by three different chemical carcinogens. Cancer Res 67:11353–11358

Nishimura J, Dewa Y, Muguruma M, Kuroiwa Y, Yasuno H, Shima T, Jin M, Takahashi M, Umemura T, Mitsumori K (2007) Effect of fenofibrate on oxidative DNA damage and on gene expression related to cell proliferation and apoptosis in rats. Toxicol Sci 97:44–54

Ohkawa H, Ohnishi N, Yagi K (1979) Assay for lipid peroxides in animal tissues by thiobarbituric acid reaction. Anal Biochem 95:351–358

Park JY, Shigenaga MK, Ames BN (1996) Induction of cytochrome P4501A1 by 2, 3, 7, 8-tetrachlorodibenzo-p-dioxin or indolo(3, 2-b)carbazole is associated with oxidative DNA damage. Proc Natl Acad Sci USA 93:2322–2327

Poulos TL, Raag R (1992) Cytochrome P450cam: crystallography, oxygen activation, and electron transfer. FASEB J 6:674–679

Raza H, Robin MA, Fang JK, Avadhani NG (2002) Multiple isoforms of mitochondrial glutathione S-transferases and their differential induction under oxidative stress. Biochem J 366:45–55

Riley RJ, Workman P (1992) DT-diaphorase and cancer chemotherapy. Biochem Pharmacol 43:1657–1669

Sanchez-Perez Y, Carrasco-Legleu C, Garcia-Cuellar C, Perez-Carreon J, Hernandez-Garcia S, Salcido-Neyoy M, Aleman-Lazarini L, Villa-Trevino S (2005) Oxidative stress in carcinogenesis. Correlation between lipid peroxidation and induction of preneoplastic lesions in rat hepatocarcinogenesis. Cancer Lett 217:25–32

Schlezinger JJ, White RD, Stegeman JJ (1999) Oxidative inactivation of cytochrome P–450 1A (CYP1A) stimulated by 3, 3′, 4, 4′-tetrachlorobiphenyl: production of reactive oxygen by vertebrate CYP1As. Mol Pharmacol 56:588–597

Schlezinger JJ, Struntz WD, Goldstone JV, Stegeman JJ (2006) Uncoupling of cytochrome P450 1A and stimulation of reactive oxygen species production by co-planar polychlorinated biphenyl congeners. Aquat Toxicol 77:422–432

Shertzer HG, Genter MB, Shen D, Nebert DW, Chen Y, Dalton TP (2006) TCDD decreases ATP levels and increases reactive oxygen production through changes in mitochondrial F(0)F(1)-ATP synthase and ubiquinone. Toxicol Appl Pharmacol 217:363–374

Shoda T, Onodera H, Takeda M, Uneyama C, Imazawa T, Takegawa K, Yasuhara K, Watanabe T, Hirose M, Mitsumori K (1999) Liver tumor promoting effects of fenbendazole in rats. Toxicol Pathol 27:553–562

Talalay P, Fahey JW, Holtzclaw WD, Prestera T, Zhang Y (1995) Chemoprotection against cancer by phase 2 enzyme induction. Toxicol Lett 82/83:173–179

Thimmulappa RK, Mai KH, Srisuma S, Kensler TW, Yamamoto M, Biswal S (2002) Identification of Nrf2-regulated genes induced by the chemopreventive agent sulforaphane by oligonucleotide microarray. Cancer Res 62:5196–5203

Trush MA, Kensler TW (1991) An overview of the relationship between oxidative stress and chemical carcinogenesis. Free Radic Biol Med 10:201–209

Umemura T, Kuroiwa Y, Kitamura Y, Ishii Y, Kanki K, Kodama Y, Itoh K, Yamamoto M, Nishikawa A, Hirose M (2006) A crucial role of Nrf2 in in vivo defense against oxidative damage by an environmental pollutant, pentachlorophenol. Toxicol Sci 90:111–119

Velik J, Baliharova V, Fink-Gremmels J, Bull S, Lamka J, Skalova L (2004) Benzimidazole drugs and modulation of biotransformation enzymes. Res Vet Sci 76:95–108

WHO (1991) Residues of some veterinary drugs in animals and foods. Monographs prepared by the thirty-eighth meeting of the joint FAO/WHO Expert Committee on food additives. FAO Food Nutr Pap 41:1–136

WHO (1999) Evaluation of certain veterinary drug residues in food. Fiftieth report of the joint FAO/WHO Expert Committee on Food Additives. World Health Organ Tech Rep Ser 888:1–95

Wiseman H, Halliwell B (1996) Damage to DNA by reactive oxygen and nitrogen species: role in inflammatory disease and progression to cancer. Biochem J 313:17–29

Yoshihara S, Makishima M, Suzuki N, Ohta S (2001) Metabolic activation of bisphenol A by rat liver S9 fraction. Toxicol Sci 62:221–227

Carcinogenesis vol.29 no.11 pp.2218–2226, 2008
doi:10.1093/carcin/bgn135
Advance Access publication June 26, 2008

Cellular distributions of molecules with altered expression specific to the tumor promotion process from the early stage in a rat two-stage hepatocarcinogenesis model

Miwa Takahashi[1], Makoto Shibutani[1,3,*], Gye-Hyeong Woo[1], Kaoru Inoue[1], Hitoshi Fujimoto[1], Katsuhide Igarashi[2], Jun Kanno[2], Masao Hirose[1,4] and Akiyoshi Nishikawa[1]

[1]Division of Pathology and [2]Division of Molecular Toxicology, National Institute of Health Sciences, 1-18-1 Kamiyoga, Setagaya-ku, Tokyo 158-8501, Japan, [3]Laboratory of Veterinary Pathology, Tokyo University of Agriculture and Technology, 3-5-8 Saiwai-cho, Fuchu City, Tokyo 183-8509, Japan and [4]Food Safety Commission, 2-13-10 Prudential Tower 6th Floor, Nagata-cho, Chiyoda-ku, Tokyo 100-8989, Japan

*To whom correspondence should be addressed. Tel: +81 42 367 5874; Fax: +81 42 367 5771;
Email: mshibuta@cc.tuat.ac.jp

A global gene expression profiling specific to the early process of tumor promotion by fenbendazole (FB) or phenobarbital (PB) in a rat two-stage hepatocarcinogenesis model revealed 33 genes to show altered expression in common with both chemicals. The immunohistochemical distribution of transferrin receptor (Tfrc), nuclear receptor subfamily 0, group B, member 2 (*Nr0b2*) and minichromosome maintenance deficient 6 (MCM6), included in the altered expression profile, were therefore examined in FB- and PB-induced proliferative lesions at both early and late stages of tumor promotion. In addition, immunoexpression of transforming growth factor β receptor (TGFβR) I, TGFβRII, phosphatase and tensin homolog deleted on chromosome 10 (PTEN) and phosphorylated phosphatase and tensin homolog deleted on chromosome 10 (pPTEN) was also examined. In the early stage, most hepatocellular foci positive for glutathione *S*-transferase placental form (GST-P) showed co-expression of TGFβRI and lack of PTEN and pPTEN, some GST-P-positive foci co-expressing Tfrc and *Nr0b2*. In the late stage, selective expression of TGFβRI, but not TGFβRII, was also observed in many adenomas and carcinomas consistently expressing GST-P. *Nr0b2* was variably expressed in the proliferative lesions, irrespective of the carcinogenic stage. Like the GST-P-positive foci, adenomas and carcinomas consistently lacked PTEN and pPTEN. Expression of Tfrc and MCM6 was increased in parallel with the carcinogenic stage. In conclusion, loss of PTEN and dysregulation of transforming growth factor β signaling can be considered to be involved in rat hepatocarcinogenesis from early stages. Selective expression of Tfrc in proliferative lesions suggests an involvement of changes in iron homeostasis during the process of tumor promotion/progression driven by FB or PB.

Introduction

Molecular events in multistep carcinogenesis due to non-genotoxic carcinogens remain largely unclear. Currently, although acceptable daily intake levels have been established for non-genotoxic carcinogens such as food additives, pesticides and animal drugs contained in food, a more thorough understanding of the mechanisms of non-genotoxic carcinogenesis is needed to secure human health. The carcinogens in question usually exert tumor-promoting activity of target organs in two-stage carcinogenesis models in rodents, and signatures of carcinogenic responses can be determined by analysis of preneoplastic lesions generated at early stages of tumor promotion. This is the rationale for global gene expression profiling focusing on early stages of carcinogenesis for elucidation of putative molecular mechanisms responsible for early carcinogenic actions.

The glutathione *S*-transferase placental form (GST-P) has been identified as a reliable marker for preneoplastic lesions as end points in rat liver for rapid detection of carcinogenic agents (1). However, it is known that only a small proportion of such foci actually progress to liver tumors. In a recent report, it is suggested that double-positive foci for GST-P and transforming growth factor (TGF) α in the early stages of rat hepatocarcinogenesis may be most probably to develop into tumors with promotion (2). Also, dysregulation of TGFβ signaling, such as altered expression of transforming growth factor β receptors (TGFβRs), has been considered to play a critical role in the promotion and progression stages of hepatocarcinogenesis, both in humans and rodents (3–5). It has been reported that expression of TGFβ and its receptors is altered in preneoplastic lesions in rat liver during the tumor promotion stage (6,7). Phosphatase and tensin homolog deleted on chromosome 10 (*PTEN*) is a tumor suppressor gene involved in a variety of tumor types, and down-regulation of PTEN expression may contribute to the development of human hepatocellular carcinomas (8,9). In rats, clear roles of PTEN in hepatocarcinogenesis remain to be explored (10).

In the present study, to determine molecular mechanisms involved in the non-genotoxic hepatocarcinogenesis in rat liver, we performed a global expression profiling of mRNAs specific to the early stage of tumor promotion by fenbendazole (FB), an anti-helminthic drug (11), and phenobarbital (PB), a well-studied hepatocarcinogenesis promoter (12), in a rat two-stage hepatocarcinogenesis model using a medium-term liver bioassay (13,14). Reduction of connexin 32 in centrilobular hepatocytes as well as cytochrome P450 (CYP) 1A2 induction have been suggested to be involved in the mechanism of liver tumor promotion by FB (11). PB is also known to induce CYP enzymes, particularly CYP2B1/2 and CYP3A2 (15). It has been reported that PB inhibits cell-to-cell communication, stimulates proliferation and inhibits apoptosis of hepatocytes in preneoplastic foci (16). In addition, increased oxidative stresses due to activation of detoxifying enzymes are suggested to be responsible for hepatocarcinogenesis by PB (15). Based on the expression profiles obtained in the present study, we further examined cellular localization of molecules that showed altered expression at the early stage of hepatocarcinogenesis by FB and PB in common, such as transferrin receptor (Tfrc), nuclear receptor subfamily 0, group B, member 2 (*Nr0b2*) and minichromosome maintenance deficient 6 (MCM6), immunohistochemically in the FB- or PB-induced hepatocellular adenomas and carcinomas as well as in the liver cell foci. We also additionally examined changes in immunolocalization of TGFβRs, PTEN and phosphorylated phosphatase and tensin homolog deleted on chromosome 10 (pPTEN) during the course of hepatocarcinogenesis.

Abbreviations: CYP, cytochrome P450; DEN, *N*-diethylnitrosamine; FB, fenbendazole; GST-P, glutathione *S*-transferase placental form; MCM6, minichromosome maintenance deficient 6; *Nr0b2*, nuclear receptor subfamily 0, group B, member 2; PH, partial hepatectomy; PB, phenobarbital; PTEN, phosphatase and tensin homolog deleted on chromosome 10; pPTEN, phosphorylated phosphatase and tensin homolog deleted on chromosome 10; RT, reverse transcription; PCR, polymerase chain reaction; Tfrc, transferrin receptor; TGF, transforming growth factor; TGFβR, transforming growth factor β receptor.

Materials and methods

Chemicals

FB (CAS No. 43210-67-9) was purchased from Sigma-Aldrich Japan K.K. (Tokyo, Japan). PB sodium (CAS No. 57-30-7) was obtained from Wako Pure Chemicals Industries (Osaka, Japan) and *N*-diethylnitrosamine (DEN, CAS No. 55-18-5) from Tokyo Chemical Industry, Ltd (Tokyo, Japan).

Animal experiments

Male 5-week-old F344/DuCrj rats were purchased from Charles River Japan (Kanagawa, Japan) and acclimatized on powdered basal diet (CRF-1; Oriental Yeast, Tokyo, Japan) and tap water *ad libitum* for 1 week. They were housed in

polycarbonate cages with sterilized softwood chips as bedding in a barrier-maintained animal room conditioned at 23–25°C and 50–60% humidity on a 12-h light/dark cycle.

In the experiment 1, for gene expression profiling and immunohistochemical examination of rat livers at the early stage of tumor promotion, a two-stage hepatocarcinogenesis model was employed using a medium-term liver bioassay (13,14). A total of 120 rats were divided into 10 groups. Seven groups were initiated with a single intraperitoneal injection of DEN (200 mg/kg, dissolved in saline) and the others received a single intraperitoneal injection of saline vehicle alone. Two weeks later, rats in the DEN-initiated groups were fed diet containing FB 400, 1200 or 3600 p.p.m. (DEN + FB groups) or PB 56, 167 or 500 p.p.m. (DEN + PB groups) or basal diet (DEN-alone group). The rats without initiation were given FB 3600 p.p.m. (FB group) or PB 500 p.p.m. (PB group) or basal diet (untreated control group). The highest doses of FB or PB were set as concentrations that exhibited tumor promotion effects in rat liver in previous reports (FB, 11; PB, 12). The animals were subjected to two-thirds partial hepatectomy (PH) at week 3 except for sham surgery in the untreated control group. At week 8, the animals were killed under deep ether anesthesia by exsanguination, and their livers were immediately removed and weighed. The liver tissues were immersed in RNAlater® solution (Ambion, Austin, TX) at 4°C overnight and then stored at −80°C until use after removing the solution. In addition, liver slices were fixed in 10% phosphate-buffered formalin (pH 7.4) and processed routinely for histopathological examination.

In experiment 2, to investigate immunohistochemical distribution of selected proteins in late stages of tumor promotion, 35 animals each initiated with DEN were given diet containing FB 3600 p.p.m. or PB 500 p.p.m. from 2 weeks after initiation. They were subjected to PH at week 3 and maintained until week 59 to induce hepatocellular tumors. The livers of surviving animals were removed and the liver slices containing neoplastic lesions grossly (1 slice per a rat) were fixed in 10% phosphate-buffered formalin and prepared for histopathological examination.

The treatment groups in experiments 1 and 2 are summarized in supplementary Table S1 (available at *Carcinogenesis* and Online). The animal protocol was reviewed and approved by the Animal Care and Use Committee of the National Institute of Health Sciences, Japan.

RNA preparation

For microarray analysis and subsequent real-time reverse transcription (RT)–polymerase chain reaction (PCR) analysis, total RNA was isolated from livers of four rats in each group in experiment 1 using an RNeasy Mini Kit (QIAGEN K.K., Tokyo, Japan). Concentrations and quality of RNA were determined with a RiboGreen RNA Quantitation Kit (Molecular Probes, Eugene, OR) and an RNA 6000 Nano LabChip Kit (Agilent Technologies Japan, Ltd, Tokyo, Japan), respectively.

Microarray analysis

Five microgram aliquots of total RNA were subjected to amplification, consisting of RT and subsequent *in vitro* one-step transcription, using a MessageAmp™ II aRNA amplification Kit (Ambion) with a T7 oligo (dT) primer, according to the manufacturer's protocol. During the *in vitro* transcription, generated aRNAs were labeled with biotin-16-UTP and biotin-11-CTP (Enzo Biochem, Farmingdale, NY). Aliquots of 20 μg of biotinylated aRNA were fragmented, hybridized with a GeneChip® Rat Genome 230 2.0 Array (Affymetrix, Santa Clara, CA) at 45°C for 18 h, stained with streptavidin–*R*-phycoerythrin conjugates (Molecular Probes) and then scanned with a GeneChip® Scanner 3000 (Affymetrix).

Selection of genes and normalization of expression data were performed using GeneSpring® software (version 7.2; Silicon Genetics, Redwood City, CA). To normalize chip-wide variation in intensity, per chip normalization was performed by dividing the signal strength for each gene with the level of the 50th percentile of the measurement in the chip, and each gene was divided by the average intensity in the samples of untreated control or DEN-alone groups. Genes showing expression change with differences at least 2-fold in magnitude from the untreated control or DEN-alone groups, as well as the 'presence' signal in >¾ of samples in the group showing higher expression values in comparison were selected. To obtain an expression profile specific to the early stages of tumor promotion by FB or PB in the rat two-stage hepatocarcinogenesis model, genes showing altered expression in the FB-, PB- or DEN-alone group as compared with the untreated control group were selected first. Next, genes showing expression changes in the DEN + FB 3600 p.p.m. or DEN + PB 500 p.p.m. as compared with the DEN-alone group were selected. Then, genes showing altered expression specific to the promotion with FB were collected by subtracting the population of genes showing expression changes in the FB and DEN-alone groups from that showing expression changes with DEN + FB 3600 p.p.m. Similarly, genes showing altered expression specific to PB promotion were identified by subtracting the population of genes showing expression changes in the PB- and DEN-alone groups from that showing expression changes in the DEN + PB 500 p.p.m. Genes showing altered expression in common with both chemicals were also selected. Among genes selected at the highest dose of each carcinogen, those showing dose-related expression changes were further identified by analysis of expression levels with the low- and middle-dose groups for each chemical.

Real-time RT–PCR

Quantitative real-time RT–PCR was performed for confirmation of expression values obtained with microarrays using an ABI Prism 7900HT (Applied Biosystems Japan Ltd, Tokyo, Japan). The following genes were selected as targets: alcohol dehydrogenase 1 (*Adh1*), syntaxin 6 (*Stx6*), pregnancy-induced growth inhibitor (*Oki38*), v-maf musculoaponeurotic fibrosarcoma oncogene family, protein B (*Mafb*), *Nr0b2*, dual specificity phosphatase 1 (*Dusp1*), *Axin2* and *Igfbp1*. One microgram of total RNA was applied to RT with a High-Capacity cDNA Archive Kit (Applied Biosystems Japan Ltd) in a 100-μl total reaction volume. For real-time PCR analysis, ABI Assays-on-Demand™ TaqMan probe and primer sets from Applied Biosystems (available at https://products.appliedbiosystems.com/ab/en/US/adirect/ab?cmd=catNavigate2&catID=601267/) were used except for *Adh1*. Real-time PCR was performed in a 50-μl reaction volume using the TaqMan probe detection system (Applied Biosystems Japan Ltd) with specific primers, the corresponding TaqMan® MGB probes (FAM™ dye labeled) and RT products. For *Adh1*, the primer sets were designed using Primer Express® software (version 2.0; Applied Biosystems Japan Ltd), and the sequences were TTG AAG GAA ACA ACT CCA TAT TCA TT (forward) and CAT GGC CGC TCT GCT TCT A (reverse). Amplified transcript levels were measured with the SYBR Green detection system in a 50-μl reaction mixture containing SYBR® Green PCR Master Mix (Applied Biosystems Japan Ltd), target primers and RT products. For quantification of expression data, a standard curve method was applied. Expression values were normalized to two housekeeping genes, glyceraldehyde 3-phosphate dehydrogenase and hypoxanthine–guanine phosphoribosyltransferase.

Immunohistochemistry

Formalin-fixed, paraffin-embedded liver sections were subjected to immunohistochemistry utilizing a VECTASTAIN® Elite ABC Kit (Vector Laboratories, Burlingame, CA) with 3,3'-diaminobenzidine/H_2O_2 as the chromogen. Rabbit polyclonal antibodies against GST-P (MBL, Nagoya, Japan; Catalog No. 311, 1:1000) were applied for all liver sections obtained at both 6 and 57 weeks of tumor promotion. Serial sections of eight rats of the untreated control, DEN-alone, DEN + FB 3600 p.p.m. and DEN + PB 500 p.p.m. groups at week 6 of promotion as well as all the hepatocellular tumors generated after promotion with FB or PB were subjected to immunohistochemistry for Tfrc (mouse monoclonal antibody, Zymed Laboratories, South San Francisco, CA; Catalog No. 13-6800, 1:200), *Nr0b2* (rabbit polyclonal antibody; MBL; Catalog No. LS-A5411, 1:200), MCM6 (rabbit polyclonal antibody; GeneTex, San Antonio, TX; Catalog No. GTX24458, 1:200), TGFβRI (rabbit polyclonal antibody, Santa Cruz Biotechnology, Santa Cruz, CA; Catalog No. sc-398, 1:100), TGFβRII (rabbit polyclonal antibody, Santa Cruz Biotechnology; Catalog No. sc-220, 1:100), PTEN (rabbit polyclonal antibody; Cell Signaling Technology, MA; Catalog No. 9559, 1:100) and pPTEN (rabbit polyclonal antibody; Cell Signaling Technology; Catalog No. 9551, 1:50). pPTEN is an inactive form of PTEN and the PTEN antibody detects endogenous levels of total PTEN.

For antigen retrieval, the sections were heated in 10 mM citrate buffer by autoclaving for 10 min before incubation with the TGFβRI and MCM6 antibodies or for 20 min before incubation for PTEN and pPTEN. In the *Nr0b2*, Trfc and TGFβRII cases, sections were heated by microwave for 10 min before incubation.

Analysis of immunolocalization

The numbers and areas of GST-P-positive foci and the total areas of livers at week 6 of tumor promotion were measured using an Image Processor for Analytical Pathology (IPAP-WIN; Sumika Technoservice, Osaka, Japan), and then the values per unit area (cm^2) of liver section were calculated. Cellular localization of immunohistochemically stained molecules was evaluated in relation with GST-P-positive foci and neoplastic lesions using serial sections without applying double-labeling experiments with GST-P. For evaluation of the immunoreactivity of Tfrc and *Nr0b2* in liver cells outside GST-P-positive foci at 6 weeks of promotion, staining intensity was scored as 0 (none), 1 (slight), 2 (moderate) and 3 (strong) by observation of five randomly selected areas/rat at 200-fold magnification. For evaluation of the expression of TGFβRI, TGFβRII, PTEN, pPTEN, Tfrc and *Nr0b2* in proliferative lesions (GST-P-positive foci at both 6 and 57 weeks; hepatocellular adenomas and carcinomas at 57 weeks), immunoreactivity was classified as increased, unchanged or decreased as compared with the expression levels of surrounding

liver cells. Numbers of MCM6-positive cells and total number of liver cells were counted by observation of five randomly selected areas/rat at 200-fold magnification at week 6 and counted in individual GST-P-positive foci, adenomas and carcinomas at 57 weeks, and then, MCM6-positive cell index was calculated.

Statistical analysis

Data for the numbers and areas of GST-P-positive foci were assessed by one-way analysis of variance or the Kruskal–Wallis test following Bartlett's test. When statistically significant differences were indicated, the Dunnett's multiple test was employed for comparison with the DEN-alone group. The data for gene expression levels from real-time RT–PCR analysis and MCM6-positive cell indices were analyzed by the Student's or Welch's *t*-test following a test for equal variance. For grading immunohistochemical findings, scores of Tfrc and *Nr0b2* were analyzed with the Mann–Whitney's *U*-test between the DEN-alone group and DEN + FB or DEN + PB groups. For the microarray data, statistical analysis was performed with GeneSpring® software, and the significance of gene expression changes was analyzed by the Student's *t*-test or analysis of variance between the DEN-alone and DEN + FB or DEN + PB groups.

Results

Microarray analysis

In all, 33 genes (15 genes up-regulated and 18 genes down-regulated) were identified as showing altered expression at week 6 of tumor promotion by both FB and PB (Table I). Examples showing dose-related expression changes numbered 18 and 32 in the DEN + FB and DEN + PB groups, respectively (supplementary Tables S2 and S3 are available at *Carcinogenesis* and Online). Among these, there were several whose products are involved in suppression of cell proliferation, such as *Okl38* (17), protein arginine *N*-methyltransferase 5 (*Prmt5*_predicted) (18) and *Dusp1* (19). In both DEN + FB and DEN + PB groups, up-regulation of *Okl38* and down-regulation of *Dusp1* and *Mafb*, were observed dose relatedly. Particularly, *Mafb* showed down-regulation from the lowest dose of both chemicals. The results of real-time RT–PCR for validation of microarray data are summarized in Table II. Expression levels at the highest dose of promotion in each chemical were compared between the microarray and real-time RT–PCR values. In both FB- and PB-promoted liver, many expression changes were similar between the two analysis systems, except for changes of *Stx6*. In addition, a low magnitude of alteration was found for *Adh1* by real-time RT–PCR in the PB-promoted liver.

Since up-regulation of *MCM6*, which is involved in DNA replication and reported as a marker of proliferating cells (20), was found in the DEN + FB 3600 p.p.m. group, we selected MCM6 for immunohistochemical analysis to detect cell proliferation activity. Among genes showing altered expression specific to the early stages of tumor

Table I. List of genes showing up- or down-regulation common to FB and PB promotion in the liver after 6 weeks exposure using a two-stage hepatocarcinogenesis model (≥2-fold, ≤0.5-fold)

Accession number	Gene title	Symbol	DEN + FB 3600 p.p.m.	DEN + PB 500 p.p.m.
Up-regulated (15 genes)				
AI639412	*Similar to asporin precursor*	*LOC306805*	4.08[a]*	2.24*
AA817761	*Alcohol dehydrogenase 1 (class I)*	*Adh1*	3.71**	2.01*
AY081218	*Pregnancy-induced growth inhibitor*	*Okl38*	3.48**	3.65**
NM_031665	*Syntaxin 6*	*Stx6*	3.45*	3.08**
AI410262	*EST*	—	2.77*	2.40*
AI171656	*Bicaudal C homolog 1 (Drosophila)*	*Bicc1_predicted*	2.71**	2.54**
AW527797	*EST*	—	2.63	2.66
AW435169	*Ab2-427*	*LOC500084*	2.52*	2.79**
BE112720	*Protein arginine N*-methyltransferase 5	*Prmt5_predicted*	2.42**	1.98**
BF417032	*Transferrin receptor*	*Tfrc*	2.40**	2.13*
(M58040)	*(Transferrin receptor)*	*(Tfrc)*	(2.33)**	(2.15)**
NM_031512	*Interleukin 1 beta*	*Il1b*	2.36**	2.14*
BG380736	*Similar to hepatocellular carcinoma-associated antigen 58 homolog*	*RGD1305020_predicted*	2.26**	2.48**
AI511280	*Similar to outer dense fiber of sperm tails 2-like*	*LOC685425*	2.18**	2.26*
AA891521	*Spermatogenesis associated 9*	*Spata9_predicted*	2.03*	2.38*
AW521797	*Similar to chromosome 18 open reading frame 54*	*LOC361346*	2.03*	1.60
Down-regulated (18 genes)				
BG374180	*EST*	—	0.21	0.45
AW530361	*Protein phosphatase 1, regulatory (inhibitor) subunit 3C*	*Ppp1r3c*	0.22*	0.39
(BM390827)	*[Protein phosphatase 1, regulatory (inhibitor) subunit 3C]*	*(Ppp1r3c)*	(0.24)*	(0.31)
U56241	*v-maf musculoaponeurotic fibrosarcoma oncogene family, protein B (avian)*	*Mafb*	0.29**	0.45*
BI285940	*EST*	—	0.30*	0.35*
AA956038	*EST*	—	0.33**	0.39*
BE120455	—	—	0.37*	0.38*
NM_057133	*Nuclear receptor subfamily 0, group B, member 2*	*Nr0b2*	0.40*	0.31*
BF391129	*Progressive ankylosis homolog (mouse)*	*Ank*	0.41*	0.50
BE110108	*Dual specificity phosphatase 1*	*Dusp1*	0.41*	0.44
(U02553)	*(Dual specificity phosphatase 1)*	*(Dusp1)*	(0.44)**	(0.44)*
BF552826	*Similar to RIKEN cDNA 2310057N15*	*RGD1562078_predicted*	0.41*	0.43*
BF393046	*EST*	—	0.43*	0.47**
AW141081	*Stanniocalcin 1*	*Stc1*	0.43*	0.40**
BF400220	*Transgelin 3*	*Tagln3*	0.44*	0.44**
AI044898	*Similar to Myb protein P42POP*	*RGD1565160_predicted*	0.44**	0.50**
BI291457	*EST*	—	0.46	0.62
AW252251	*EST*	—	0.49*	0.42
AA900870	*Talin 1*	*Tln1*	0.51*	0.53
BG371725	*Zinc finger and BTB domain containing 16*	*Zbtb16*	0.52*	0.10

EST, expressed sequence tag.
[a]Values are fold change with the expression level in the DEN-alone group set as 1.
*$P < 0.05$ versus DEN alone (Student's *t*-test).
**$P < 0.01$ versus DEN alone (Student's *t*-test).

Table II. Validation of microarray data by real-time RT–PCR

Gene symbol	DEN + FB 3600 p.p.m.			DEN + PB 500 p.p.m.		
	Microarray	Real-time RT–PCR normalized to		Microarray	Real-time RT–PCR normalized to	
		HPRT	GAPDH		HPRT	GAPDH
Adh1	3.71 ± 0.83[b]	3.65 ± 0.63[d]	3.64 ± 0.52[d]	2.01 ± 0.52[a]	1.32 ± 0.46	1.53 ± 0.73
Stx6	3.45 ± 1.18[a]	1.73 ± 0.44[c]	1.75 ± 0.44[c]	3.08 ± 0.63[b]	0.84 ± 0.50	0.99 ± 0.73
Okl38	3.48 ± 0.64[b]	2.40 ± 0.63[d]	2.37 ± 0.61[d]	3.65 ± 0.53[b]	1.77 ± 0.24[d]	2.00 ± 0.38[d]
Maf b	0.29 ± 0.04[b]	0.29 ± 0.03[c]	0.30 ± 0.03[c]	0.45 ± 0.09[a]	0.30 ± 0.06[c]	0.35 ± 0.03[c]
Nr0b2	0.40 ± 0.12[a]	0.29 ± 0.09[d]	0.28 ± 0.06[d]	0.31 ± 0.11[a]	0.16 ± 0.07[d]	0.18 ± 0.08[d]
Dusp1	0.41 ± 0.07[a]	0.32 ± 0.05[c]	0.32 ± 0.01[c]	0.44 ± 0.20	0.22 ± 0.14[d]	0.25 ± 0.16[d]
Axin2	2.38 ± 0.35[b]	2.54 ± 0.86	2.56 ± 1.04[c]	—	—	—
Igfbp1	—	—	—	0.28 ± 0.16	0.21 ± 0.23[c]	0.23 ± 0.20[c]

HPRT, hypoxanthine–guanine phosphoribosyltransferase; GAPDH, glyceraldehyde 3-phosphate dehydrogenase; Values are mean ± standard deviation ($n = 4$) with the expression level in the DEN-alone group set as 1.
[a]Significantly different from the DEN group at $P < 0.05$ (Student's *t*-test calculated by GeneSpring).
[b]Significantly different from the DEN group at $P < 0.01$ (Student's *t*-test calculated by GeneSpring).
[c]Significantly different from the DEN group at $P < 0.05$ (Student's *t*-test).
[d]Significantly different from the DEN group at $P < 0.01$ (Student's *t*-test).

promotion by both FB and PB, up-regulation of *Tfrc* and down-regulation of *Nr0b2* were observed with dose relation in the decrease of *Nr0b2* by FB (Table I; supplementary Table S2 is available at *Carcinogenesis* Online). Tfrc is a receptor for transferrin, which plays a major role in intracellular uptake of iron (21). It has been reported that expression of Tfrc and iron homeostasis are altered in preneoplastic nodules and hepatocellular tumors in rats (22,23). *Nr0b2* is an atypical orphan nuclear receptor that lacks a conventional DNA-binding domain, which acts as a co-regulator of various nuclear receptors and negatively regulates the gene expression of glucose 6-phosphatase (*G6Pase*), *CYP7A1* and *PEPCK* (24,25). In the preneoplastic foci in rat liver, it is well known that loss of G6Pase is commonly observed (26). Thus, we also selected Tfrc and *Nr0b2* for immunolocalization analysis in hepatocellular preneoplastic foci and tumors.

Immunolocalization at the early stage of tumor promotion

At week 6 of tumor promotion, the foci induced by FB or PB were predominantly of eosinophilic type and positive for GST-P (supplementary Table S4 is available at *Carcinogenesis* and Online). The numbers and areas of GST-P-positive foci were significantly increased in the DEN + FB 1200 and 3600 p.p.m. (8.04 ± 3.60 No./cm^2 and 0.68 ± 0.44 mm^2/cm^2 at 1200 p.p.m.; 22.09 ± 11.62 No./cm^2 and 5.93 ± 0.44 mm^2/cm^2 at 3600 p.p.m.) and DEN + PB 167 and 500 p.p.m. (6.90 ± 3.16 No./cm^2 and 0.50 ± 0.24 mm^2/cm^2 at 167 p.p.m.; 6.20 ± 2.66 No./cm^2 and 0.46 ± 0.26 mm^2/cm^2 at 500 p.p.m.) groups compared with the DEN-alone group (3.85 ± 2.04 No./cm^2 and 0.22 ± 0.13 mm^2/cm^2) (supplementary Table S5 is available at *Carcinogenesis* Online). In the untreated controls, FB-alone and PB-alone groups, very few GST-P-positive foci were observed, and there were no intergroup differences in numbers and areas.

Tfrc showed diffuse liver cell immunoreactivity in the untreated controls and DEN-alone groups, and increased intensity was observed in liver cells on promotion with FB or PB, in parallel with the microarray results (Figure 1A; supplementary Table S4 is available at *Carcinogenesis* Online). In addition, a small population of GST-P-positive foci exhibited strong immunoreactivity for Tfrc.

Nr0b2-positive liver cells were found diffusely in the untreated control group. Decreased numbers of *Nr0b2*-positive cells were observed in the DEN + FB 3600 p.p.m. and DEN + PB 500 p.p.m. groups, in parallel with the microarray data (Figure 1B; supplementary Table S4 is available at *Carcinogenesis* and Online). However, some liver cell foci positive for GST-P paradoxically showed increased numbers of *Nr0b2*-positive cells as compared with surrounding liver cells.

MCM6-positive cells were detected mainly in regenerative nodules including oval cells in the DEN + FB 3600 p.p.m. group, and their numbers were significantly increased in this group as compared with the DEN-alone group (Figure 1C).

TGFβRI and TGFβRII were immunolocalized in normal liver cells diffusely but weakly in all groups, including untreated controls (supplementary Table S4 is available at *Carcinogenesis* Online). Many GST-P-positive foci showed intense immunoreactivity for TGFβRI, especially in the DEN + FB 3600 p.p.m. group (Figure 2A). In contrast, very small populations of foci showed increased or decreased immunoreactivity for TGFβRII. PTEN and pPTEN immunoreactivity was diffusely but weakly observed in normal liver cells in all groups, including untreated controls. It was generally lacking in foci (Figure 2A; supplementary Table S4 is available at *Carcinogenesis* Online). On co-localization analysis of each molecule in association with GST-P positivity using serial sections, increased immunoreactivity of TGFβRI and decreased immunoreactivity of PTEN and pPTEN were found in most GST-P-positive foci compared with surrounding liver cells in the DEN + FB 3600 p.p.m. group. Some foci also showed co-expression of Tfrc and *Nr0b2* (Figure 2B). In the DEN + PB group, although similar immunolocalization changes to FB group were observed for these molecules, rates of foci showing altered immunoreactivity were lower than those in the DEN + FB group.

Immunolocalization at the late stage of tumor promotion

Many adenomas and carcinomas were obtained after promotion by FB or PB for 57 weeks. Most adenomas exhibited eosinophilic cytoplasm and solid growth, and carcinomas frequently showed trabecular and solid growth patterns. Foci observed at the late stage were mostly eosinophilic, but basophilic and clear cell types were also found. There were no major differences between the incidence and histological types of proliferative lesions induced by FB or PB.

All adenomas and carcinomas were positive for GST-P, although a small subset of foci, such as the basophilic type, appeared negative (Figure 3; supplementary Table S4 is available at *Carcinogenesis* Online). The immunoreactivity of TGFβRI was increased in the proliferative lesions in comparison with surrounding liver cells, and the percentages of lesions strongly expressing TGFβRI were increased in adenomas and carcinomas, in both FB and PB groups. Localized expression of TGFβRII in proliferative lesions was largely lacking, although a small proportion of lesions showed increased or decreased immunoreactivity. *Nr0b2* was variably positive in the proliferative lesions, without relation to development from foci to carcinomas. PTEN and pPTEN were weakly positive in the liver cells outside the proliferative lesions, but were consistently lacking in FB- and PB-induced foci, adenomas and carcinomas. Immunoreactivity of Tfrc and MCM6 increased in parallel with the stage of lesion development.

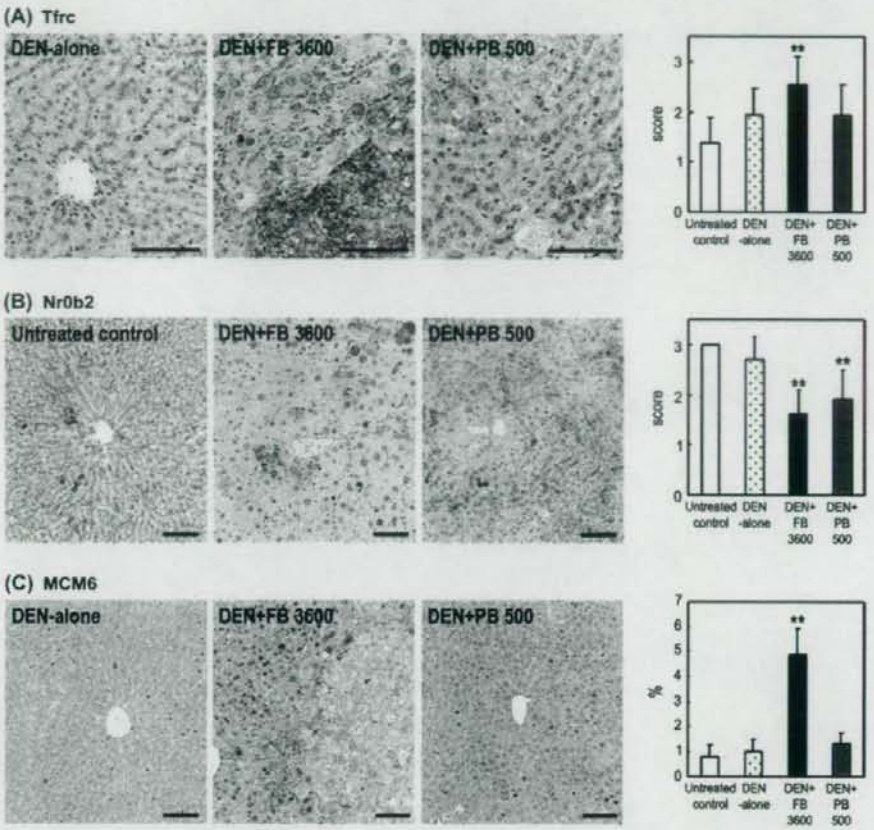

Fig. 1. Immunohistochemical distributions of Tfrc, *Nr0b2* and MCM6 in liver cells after promotion by FB or PB for 6 weeks. (**A**) Tfrc in the DEN-alone, DEN + FB 3600 p.p.m. and DEN + PB 500 p.p.m. groups. Note fine granular Tfrc immunoreactivity in the cytoplasm of liver cells with diffuse cellular distribution in the DEN-alone group. Increased intensity of Tfrc immunoreactivity is evident after promotion with FB and PB. A liver cell focus positive for GST-P exhibits strong immunoreactivity. Bar = 100 μm. The graph shows scores (mean + standard deviation) for Tfrc staining intensity. $^{**}P < 0.01$ versus DEN-alone group (Mann–Whitney's *U*-test). (**B**) *Nr0b2* in the untreated control, DEN + FB 3600 p.p.m. and DEN + PB 500 p.p.m. groups. *Nr0b2* was found diffusely in the cytoplasm of liver cells in the untreated control group, and decreased numbers of *Nr0b2*-positive cells were observed in the DEN + FB 3600 p.p.m. and DEN + PB 500 p.p.m. groups. Bar = 100 μm. $^{**}P < 0.01$ versus DEN-alone group (Mann–Whitney's *U*-test). (**C**) MCM6 in the DEN-alone, DEN + FB 3600 p.p.m. and DEN + PB 500 p.p.m. groups. MCM6-positive cells with nuclear immunoreactivity were sparsely detected in the untreated control, DEN-alone and DEN + PB 500 p.p.m. groups. In the DEN + FB 3600 p.p.m. group, MCM6-positive cells were detected mainly in regenerative nodules including oval cells. Bar = 100 μm. $^{**}P < 0.01$ versus DEN-alone group (Welch's *t*-test).

MCM6-positive cell indices did not differ in relation with the immunoreactive patterns of TGFβRI or TGFβRII in each type of proliferative lesion in either DEN + FB or DEN + PB group, although carcinomas showed particular variability (Figure 4). Foci and adenomas showing different expression patterns of *Nr0b2* did not show obvious variation in the MCM6-positive cell index. On the other hand, carcinomas showing decreased immunoreactivity of *Nr0b2* exhibited higher MCM6-positive cell indices as compared with those showing unchanged expression of this molecule as compared with surrounding liver cells in the DEN + PB group. Although statistically non-significant, a similar tendency was also observed in the DEN + FB group. In both DEN + FB and DEN + PB groups, MCM6-positive cell indices in adenomas or carcinomas lacking PTEN and pPTEN immunoreactivity were lower than in the corresponding lesions showing unchanged expression of these antigens as compared with surrounding liver cells (DEN + PB group: significantly different for pPTEN in adenomas; DEN + FB group: significantly different for PTEN and pPTEN in carcinomas). There was an increasing tendency for MCM6-positive cell indices in adenomas and carcinomas that showed increased immunoreactivity of Tfrc as compared with those in the corresponding lesions showing unchanged expression in both DEN + FB and DEN + PB groups, but it was statistically non-significant.

Discussion

Both FB and PB are known to induce CYPs, and it has been suggested that effects such as inhibition of cell-to-cell communication and oxidative stress are involved in their mechanisms of carcinogenic action (11,15,16). In the present study, we subtracted gene clusters simply responding to FB and PB alone as well as those responding to initiation and PH from those showing altered expression after initiation plus PH and following promoter treatment, and therefore, the obtained genes can be considered to play some role in the promotion process by non-genotoxic hepatocarcinogens. As a result, chemically inducible

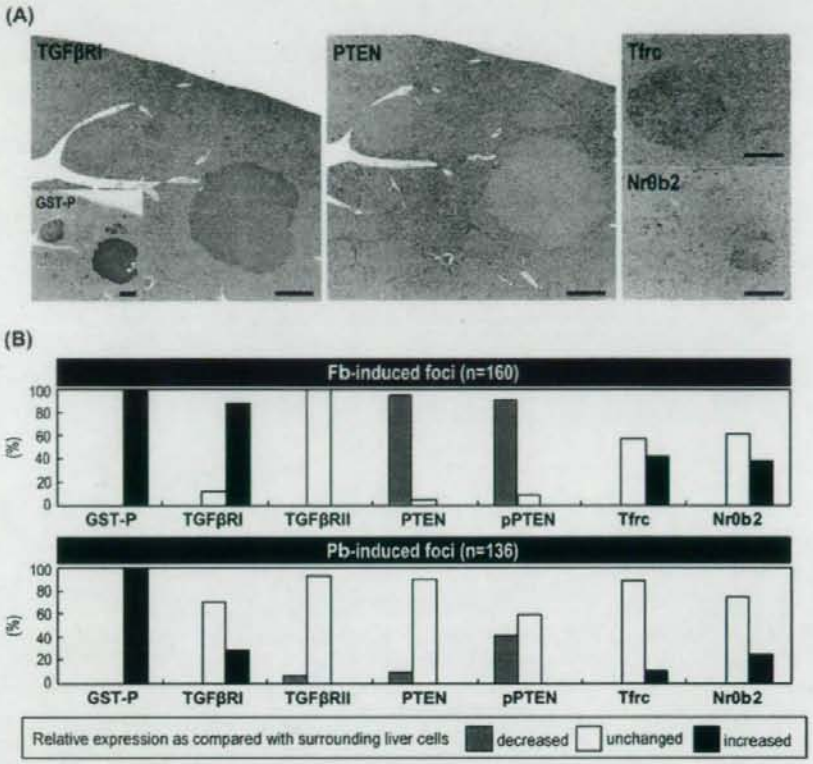

Fig. 2. (**A**) Immunohistochemical localization of TGFβRI, PTEN, Tfrc and *Nr0b2* in GST-P-positive liver cell foci after promotion by FB for 6 weeks. Increased expression of TGFβRI and decreased expression of PTEN in comparison with surrounding liver cells was found in most of GST-P-positive foci in the DEN + FB 3600 p.p.m. group, and some foci also showed co-expression of Tfrc and *Nr0b2*. Bar = 500 μm. (**B**) Immunohistochemical expression patterns of TGFβRI, TGFβRII, PTEN, pPTEN, Tfrc and *Nr0b2* in GST-P-positive liver cell foci after promotion by FB or PB for 6 weeks. Expression patterns were classified into increased, unchanged and decreased in comparison with the staining intensity in the surrounding liver cells.

genes related to drug detoxification, inhibition of cell-to-cell communication and oxidative stress responses were excluded from the expression profile. Several genes, such as *Okl38*, *Prmt5* and *Dusp1*, are known to be related to suppression of cell proliferation (17–19), suggesting that expression changes of genes toward growth suppression observed in the early stages of tumor promotion was probably a reflection of gene expression in mitotically inactive uninitiated cells that comprise the predominant cell population in the liver at this time point.

Immunohistochemical examination revealed that a subset of GST-P-positive foci exhibit increased immunolocalization of Tfrc, *Nr0b2* and TGFβRI and decreased immunoexpression of PTEN and pPTEN after promotion by FB or PB. In contrast to the promotion with FB, only a small proportion of foci showed altered expression by PB at the same early stage. This difference between FB and PB might reflect differences in the action or potential for promotion of these chemicals. However, since similar immunoexpression patterns were observed in the FB- and PB-induced tumors at the late stage, it is presumed that the role of the molecules examined here may be similar in the process of hepatocarcinogenesis. Simply, slower growth of GST-P-positive foci in the PB-promoted livers as compared with the FB-promoted ones might have lowered the chance of acquiring or losing phenotypes within the foci. It should be noted that the size of foci with PB was rather small as compared with the FB case.

Increased expression of Tfrc was observed here in a subset of GST-P-positive foci in the early stage of tumor promotion by FB or PB, and levels increased in proportion to the stage of lesion development. Iron plays an important role in many essential cell functions including the synthesis of enzymes necessary for cellular growth and metabolism, and expression of Tfrc is closely linked to the proliferation status of the cell (27). It has been reported that expression of Tfrc and iron homeostasis is altered in preneoplastic nodules and hepatocellular tumors in rats (22,23). A correlation between Tfrc expression and cell proliferation has been also shown in human breast carcinomas (28). Therefore, it is suggested that change in iron homeostasis was linked to the processes of tumor promotion and progression by FB and PB in the present study.

Nr0b2 negatively regulates transcription of G6Pase (25), and loss of G6Pase is commonly observed in preneoplastic foci in the rat liver (26). Our present finding that some liver cell foci showed positive immunoreactivity of *Nr0b2* as compared with surrounding liver cells in the early stage of tumor promotion might have caused decreased expression of G6Pase. In the late stage, *Nr0b2* was variably expressed in the proliferative lesions without relation to lesion development. Interestingly, carcinomas showing decreased expression of *Nr0b2* exhibited higher MCM6-positive cell indices in both PB- and FB-promoted livers, suggesting that the loss of *Nr0b2* may be necessary for acquisition of a malignant phenotype, different from the suggested

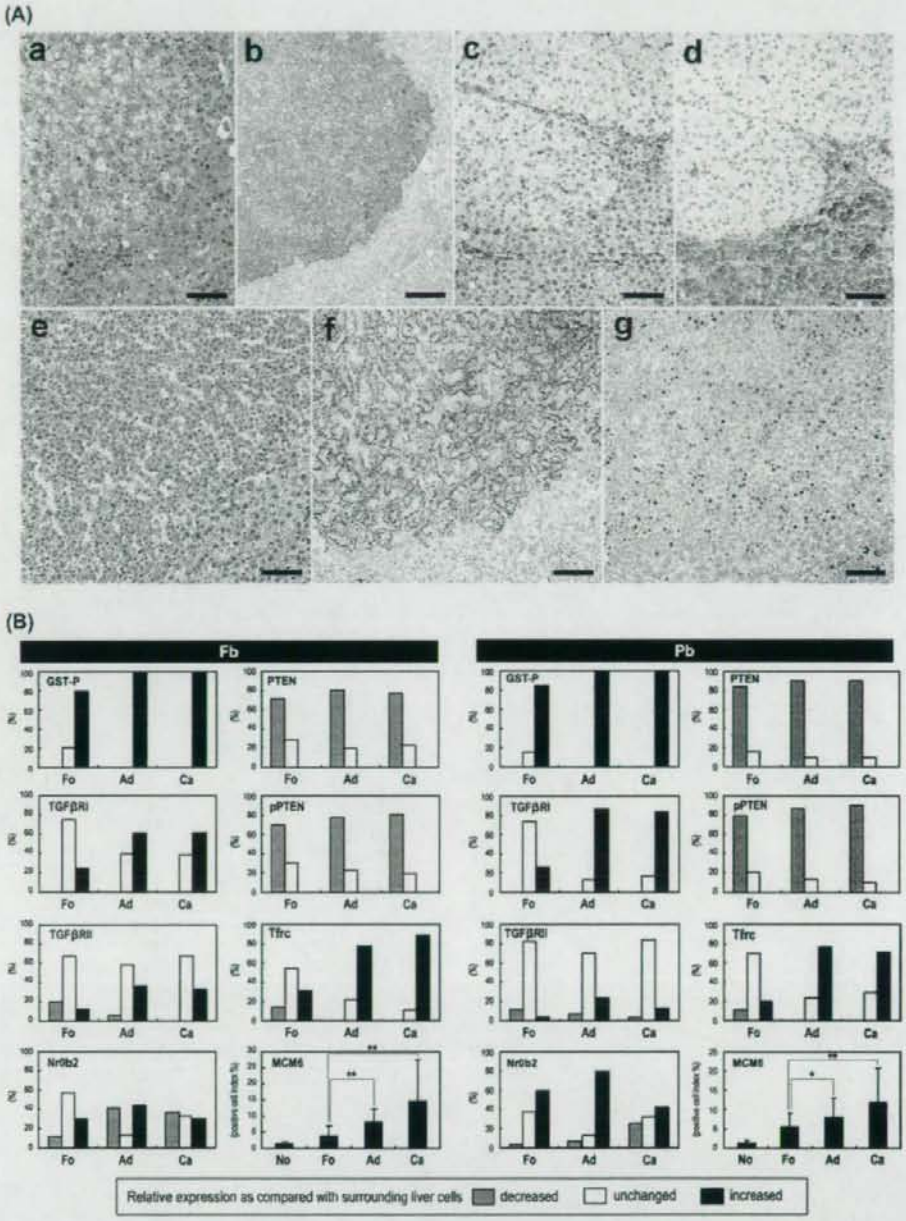

Fig. 3. (**A**) Immunohistochemical localization of TGFβRI, PTEN, *Nr0b2*, Tfrc and MCM6 in hepatocellular adenomas and carcinomas generated after promotion by FB or PB for 57 weeks. (**a**) PB-induced adenoma and hematoxylin and eosin staining. (**b**) PB-induced adenoma showing intense immunoreactivity for TGFβRI. (**c**) FB-induced adenoma lacking PTEN expression. (**d**) FB-induced adenoma showing marked decrease of *Nr0b2*-positive cells. (**e**) FB-induced carcinoma and hematoxylin and eosin staining. (**f**) FB-induced carcinoma showing strong immunoreactivity for Tfrc. (**g**) FB-induced carcinoma with a high MCM6-positive cell index. Bar = 100 μm. (**B**) Immunohistochemical expression patterns of GST-P, TGFβRI, TGFβRII, *Nr0b2*, PTEN, pPTEN and Tfrc and MCM6-positive cell indices of proliferative lesions generated after promotion by FB or PB for 57 weeks. Expression patterns were classified into increased, unchanged and decreased in comparison with the surrounding liver cells. MCM6-positive indices are shown as mean + standard deviation. $^{*}P < 0.05$ and $^{**}P < 0.01$ versus Fo (Student's *t*-test). Numbers of lesions examined: No = 16, Fo = 49, Ad = 36, Ca = 52 (FB group); No = 26, Fo = 104, Ad = 30, Ca = 31 (PB group). No, normal; Fo, focus; Ad, adenoma; Ca, carcinoma.

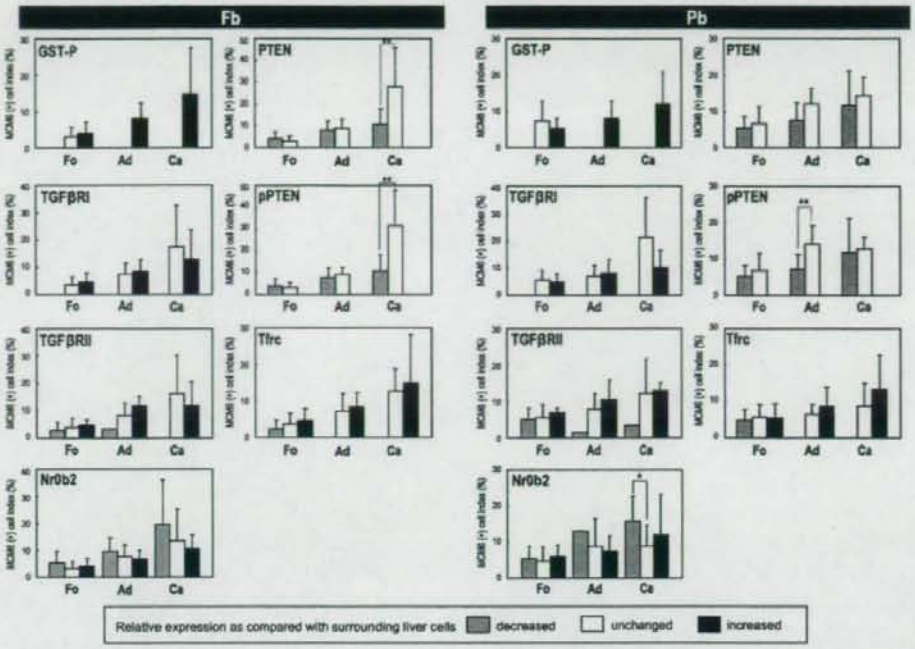

Fig. 4. MCM6-positive cell indices sorted by expression patterns for each molecule in proliferative lesions induced after promotion by FB and PB for 57 weeks. The values are mean + standard deviation. $^{*}P < 0.05$ and $^{**}P < 0.01$ versus corresponding lesions showing unchanged expression in comparison with surrounding liver cells (Student's *t*-test). Numbers of lesions examined: Fo = 49, Ad = 36, Ca = 52 (FB group); Fo = 104, Ad = 30, Ca = 31 (PB group). No, normal; Fo, focus; Ad, adenoma; Ca, carcinoma.

role for formation of G6Pase (−) foci at the early stage of tumor promotion.

TGFβ is a potent growth inhibitor in liver cells, and thus, it has been considered that down-regulation of TGFβ signaling is critical for hepatocarcinogenesis (5). There have been many studies examining expression levels of its receptors in human hepatocellular tumors, and overall, most have revealed reduction (5). In rats, decrease of TGFβRs was reported in PB-promoted hepatocellular tumors, and it is considered that down-regulation of TGFβRs might provide a selective growth advantage to tumor cells by allowing them to escape the growth inhibitory effects of TGFβ (3,29). Despite growth inhibitory effects of TGFβ signaling on liver cells, immunoreactivity of TGFβRI and TGFβRII observed in the present study was increased or unchanged, respectively, during tumor development. Although TGFβ can also act as a promoter of tumor progression during the late stage of tumorigenesis and induce tumor invasion and metastasis (30), biological effects of increased TGFβRI expression in foci from the early stage of tumor promotion cannot be unequivocally concluded. Since MCM6-positive cell indices did not differ with the levels of TGFβRI and TGFβRII, the TGFβ signaling pathway is possibly impaired in these proliferative lesions. It has been proposed that the ratio between TGFβRI and TGFβRII influences the cellular fate by controlling signaling (31). Therefore, differences in expression patterns between TGFβRI and TGFβRII in GST-P-positive lesions might lead to dysregulation of TGFβ signaling. Dysregulation of downstream effectors of TGFβ, such as smad2 and smad4, has been reported to contribute to the tumor progression during chemical carcinogenesis in rats (32). In addition, increased expression of smad7, an inhibitory downstream molecule of the TGFβ signaling, has been found in many of advanced human hepatocellular carcinomas, suggestive of its role for acquisition of resistance to TGFβ, especially in hepatocellular tumors without reduction of TGFβRs (33). Thus, further investigations of factors downstream of TGFβ signaling are needed to clarify the reason for the unexpected cellular distribution of TGFβRI and TGFβRII in relation to hepatocarcinogenesis.

In human hepatocellular carcinomas, it has been reported that expression of PTEN is reduced or absent in almost half of cases and reduced PTEN expression may be involved in pathogenesis and tumor progression (8,34). In rats, there have been only few reports of PTEN expression in the liver tumors. Silins *et al.* (10) described a subset of preneoplastic foci exhibiting a PTEN-positive phenotype and suggested there to be targeted for sphingolipid-induced apoptosis. In the present study, the levels of both PTEN and pPTEN were decreased consistently in the foci, adenomas and carcinomas, suggesting that reduction of PTEN function may be involved in rat hepatocarcinogenesis from an early stage. Involvement of the PI3 kinase pathway, including PTEN and AKT, has recently been shown in TGFβ-induced invasion during the tumor progression process (35,36), implying a possible contribution to late-stage tumor promotion. Expression of the *PTEN* gene can be suppressed by TGFβ (37). Since increased expression of TGFβRI and decreased expression of PTEN and pPTEN were often found concomitantly in the present study, further investigation of this relationship appears warranted. Although the relation to loss of tumor suppressor function is unclear, neoplastic lesions lacking PTEN/pPTEN expression in the present study exhibited lower MCM6-positive cell indices than those retaining these antigens. Some functions related to tumor progression other than proliferation might be activated in tumors lacking PTEN/pPTEN.

In conclusion, we here found 33 genes showing altered expression specific to the early stages of tumor promotion by both FB and PB in the rat two-stage hepatocarcinogenesis model using microarray technique. Immunohistochemical analysis indicated that changes of iron

homeostasis following increased expression of Tfrc, specifically in proliferative lesions, contribute to tumor promotion and progression by FB or PB. Loss of *Nr0b2* might possibly play a role in acquisition of the malignant phenotype in hepatocellular tumors. In addition, loss of PTEN and dysregulation of TGFβ signaling may be considered to be involved in rat hepatocarcinogenesis from early stages. Thus, our approaches applied here utilizing microarray analysis and following immunohistochemical screening may help searching early biomarkers of carcinogenesis. Although further studies should address roles in the processes of hepatocarcinogenesis, obtained molecules in the present study may be beneficial for detection and evaluation of non-genotoxic carcinogens that we are at risk, as well as for understanding of the mechanism of non-genotoxic carcinogenesis to secure human health.

Supplementary material

Supplementary Tables S1–S5 can be found at http://carcin.oxfordjournals.org/

Funding

Health and Labour Sciences Research Grants (Research on Food Safety) from the Ministry of Health, Labour and Welfare of Japan.

Acknowledgements

We thank Miss Tomomi Morikawa and Ayako Kaneko for their technical assistance in conducting the animal study.

References

1. Tatematsu,M. *et al.* (1985) Relative merits of immunohistochemical demonstrations of placental, A, B and C forms of glutathione S-transferase and histochemical demonstration of gamma-glutamyl transferase as markers of altered foci during liver carcinogenesis in rats. *Carcinogenesis*, **6**, 1621–1626.
2. Kitano,M. *et al.* (2006) Possible tumor development from double positive foci for TGF-α and GST-P observed in early stages on rat hepatocarcinogenesis. *Cancer Sci.*, **97**, 478–483.
3. Reisenbichler,H. *et al.* (1994) Transforming growth factor-beta receptors type I, II and III in phenobarbital-promoted rat liver tumors. *Carcinogenesis*, **15**, 2763–2767.
4. Ueno,T. *et al.* (2001) Relation of type II transforming growth factor-beta receptor to hepatic fibrosis and hepatocellular carcinoma. *Int. J. Oncol.*, **18**, 49–55.
5. Breuhahn,K. *et al.* (2006) Dysregulation of growth factor signaling in human hepatocellular carcinoma. *Oncogene*, **25**, 3787–3800.
6. Lim,I.K. *et al.* (1999) Regulation of selection of liver nodules initiated with *N*-nitrosodiethylamine and promoted with nodularin injections in Fischer 344 male rats by reciprocal expression of transforming growth factor-β1 and its receptors. *Mol. Carcinog.*, **26**, 83–92.
7. Park,D.Y. *et al.* (2001) Expression of transforming growth factor (TGF)-beta1 and TGF-beta type II receptor in preneoplastic lesions during chemical hepatocarcinogenesis of rats. *Toxicol. Pathol.*, **29**, 541–549.
8. Fabregat,I. *et al.* (2007) Survival and apoptosis: a dysregulated balance in liver cancer. *Liver Int.*, **27**, 155–162.
9. Wang,L. *et al.* (2007) Epigenetic and genetic alterations of PTEN in hepatocellular carcinoma. *Hepatol. Res.*, **37**, 389–396.
10. Silins,I. *et al.* (2006) Dietary sphingolipids suppress a subset of preneoplastic rat liver lesions exhibiting high PTEN, low phospho-Akt and high levels of ceramide species. *Food Chem. Toxicol.*, **44**, 1552–1561.
11. Shoda,T. *et al.* (1999) Liver tumor promoting effects of fenbendazole in rats. *Toxicol. Pathol*, **27**, 553–562.
12. Tatematsu,M. *et al.* (1988) Reciprocal relationship between development of glutathione S-transferase positive liver foci and proliferation of surrounding hepatocytes in rats. *Carcinogenesis*, **9**, 221–225.
13. Shirai,T. (1997) A medium-term rat liver bioassay as a rapid in vivo test for carcinogenic potential, a historical review of model development and summary of results from 291 tests. *Toxicol. Pathol.*, **25**, 453–460.
14. Ito,N. *et al.* (2000) Early detection of carcinogenic substances and modifiers in rats. *Mutat. Res.*, **462**, 209–217.
15. Kinoshita,A. *et al.* (2003) Phenobarbital at low dose exerts hormesis in rat hepatocarcinogenesis by reducing oxidative DNA damage, altering cell proliferation, apoptosis and gene expression. *Carcinogenesis*, **24**, 1389–1399.
16. Whysner,J. *et al.* (1996) Phenobarbital mechanistic data and risk assessment: enzyme induction, enhanced cell proliferation, and tumor promotion. *Pharmacol. Ther.*, **71**, 153–191.
17. Ong,C.K. *et al.* (2004) Genomic structure of human OKL38 gene and its differential expression in kidney carcinogenesis. *J. Biol. Chem.*, **279**, 743–754.
18. Gilbreth,M. *et al.* (1998) Negative regulation of mitosis in fission yeast by the shk1 interacting protein skb1 and its human homolog, Skb1Hs. *Proc. Natl Acad. Sci. USA.*, **95**, 14781–14786.
19. Brondello,J.M. *et al.* (1999) Reduced MAP kinase phosphatase-1 degradation after p42/p44MAPK-dependent phosphorylation. *Science*, **286**, 2514–2517.
20. Schrader,C. *et al.* (2005) Minichromosome maintenance protein 6, a proliferation marker superior to Ki-67 and independent predictor of survival in patients with mantle cell lymphoma. *Br. J. Cancer*, **93**, 939–945.
21. Ponka,P. *et al.* (1999) The transferrin receptor: role in health and disease. *Int. J. Biochem. Cell Biol.*, **31**, 1111–1137.
22. Pascale,R.M. *et al.* (1998) Transferrin and transferrin receptor gene expression and iron uptake in hepatocellular carcinoma in the rat. *Hepatology*, **27**, 452–461.
23. Holmström,P. *et al.* (2006) Expression of iron regulatory genes in a rat model of hepatocellular carcinoma. *Liver Int.*, **26**, 976–985.
24. Seol,W. *et al.* (1996) An orphan nuclear hormone receptor that lacks a DNA binding domain and heterodimerizes with other receptors. *Science*, **272**, 1336–1339.
25. Kim,J.Y. *et al.* (2004) Orphan nuclear receptor small heterodimer partner represses hepatocyte nuclear factor 3/Foxa transactivation via inhibition of its DNA binding. *Mol. Endocrinol.*, **18**, 2880–2894.
26. Sawaki,M. *et al.* (1990) Phenotype of preneoplastic and neoplastic liver lesions during spontaneous liver carcinogenesis of LEC rats. *Carcinogenesis*, **11**, 1857–1861.
27. Bomford,A.B. *et al.* (1985) Transferrin and its receptor: their roles in cell function. *Hepatology*, **5**, 870–875.
28. Wrba,F. *et al.* (1989) Ki-67 immunoreactivity in breast carcinomas in relation to transferrin receptor expression, estrogen receptor status and morphological criteria. An immunohistochemical study. *Oncology*, **46**, 255–259.
29. Mansbach,J.M. *et al.* (1996) Phenobarbital selectively promotes initiated cells with reduced TGF beta receptor levels. *Carcinogenesis*, **17**, 171–174.
30. Akhurst,R.J. *et al.* (2001) TGF-beta signaling in cancer—a double-edged sword. *Trends Cell Biol.*, **11**, S44–S51.
31. Huang,S.S. *et al.* (2005) TGF-beta control of cell proliferation. *J. Cell Biochem.*, **96**, 447–462.
32. Park,D.Y. *et al.* (2003) Expression and localization of the transforming growth factor-beta type I receptor and Smads in preneoplastic lesions during chemical hepatocarcinogenesis in rats. *J. Korean Med. Sci.*, **18**, 510–519.
33. Park,Y.N. *et al.* (2004) Expression of Smad7 in hepatocellular carcinoma and dysplastic nodules: resistance mechanism to transforming growth factor-beta. *Hepatogastroenterology*, **51**, 396–400.
34. Hu,T.H. *et al.* (2003) Expression and prognostic role of tumor suppressor gene PTEN/MMAC1/TEP1 in hepatocellular carcinoma. *Cancer*, **97**, 1929–1940.
35. Shigeoka,Y. *et al.* (2004) Sulindac sulfide and caffeic acid phenethyl ester suppress the motility of lung adenocarcinoma cells promoted by transforming growth factor-beta through Akt inhibition. *J. Cancer Res. Clin. Oncol.*, **130**, 146–152.
36. Hjelmeland,A.B. *et al.* (2005) Loss of phosphatase and tensin homologue increases transforming growth factor beta-mediated invasion with enhanced SMAD3 transcriptional activity. *Cancer Res.*, **65**, 11276–11281.
37. Wu,H. *et al.* (2003) PTEN signaling pathways in melanoma. *Oncogene*, **22**, 3113–3122.

Received February 23, 2008; revised May 17, 2008; accepted May 25, 2008

Toxicology 257 (2009) 46–52

Contents lists available at ScienceDirect

Toxicology

journal homepage: www.elsevier.com/locate/toxicol

Possible participation of oxidative stress in causation of cell proliferation and *in vivo* mutagenicity in kidneys of *gpt* delta rats treated with potassium bromate

Takashi Umemura[a,*], Masako Tasaki[a], Aki Kijima[a], Toshiya Okamura[a], Tomoki Inoue[a], Yuji Ishii[a], Yuta Suzuki[a], Norio Masui[b], Takehiko Nohmi[c], Akiyoshi Nishikawa[a]

[a] Division of Pathology, National Institute of Health Sciences, 1-18-1, Kamiyoga, Setagaya-ku, Tokyo 158-8501, Japan
[b] Japan SLC Co., 3371-8, Koto-chou, Nishi-ku, Hamamatsu, Schizuoka 431-1103, Japan
[c] Division of Genetics and Mutagenesis, National Institute of Health Sciences, 1-18-1, Kamiyoga, Setagaya-ku, Tokyo 158-8501, Japan

ARTICLE INFO

Article history:
Received 11 November 2008
Received in revised form 5 December 2008
Accepted 5 December 2008
Available online 14 December 2008

Keywords:
Potassium bromate
gpt delta rat
BrdU
α-Tocopherol
Sodium ascorbic acid

ABSTRACT

Clarifying the participation of oxidative stress among possible contributing factors in potassium bromate ($KBrO_3$)-induced carcinogenesis is of importance from the perspective of human health protection. In the present study, utilizing the antioxidative effects of α-tocopherol (α-TP) or sodium ascorbic acid (SAA) to attenuate oxidative stress, alterations in bromodeoxyuridine labeling indices (BrdU-LIs) and reporter gene mutations in kidneys of male and female *gpt* delta rats given $KBrO_3$ were examined. Five male and female *gpt* delta rats in each group were given $KBrO_3$ at a concentration of 500 ppm in the drinking water for 9 weeks, with 1% of α-TP or SAA administered in the diet from 1 week prior to the $KBrO_3$ treatment until the end of the experiment. Increases in 8-hydroxydeoxyguanosine levels in kidney DNA of both sexes of rats given $KBrO_3$ were significantly inhibited by SAA, but not α-TP. While BrdU-LIs in the proximal tubules of female rats were also significantly reduced by SAA, those in the males and *gpt* mutant frequencies in kidney DNA of both sexes were not affected by SAA or α-TP. Immunohistochemical and Western blot analyses for α_{2u}-globulin strongly suggested that induction of cell proliferation observed in the males might primarily result from accumulation of this protein, independent of oxidative stress. The overall data indicated that while oxidative stress well correlates with induction of cell proliferation in females, its role in males and in generation of *in vivo* mutagenicity by $KBrO_3$ in both sexes is limited.

1. Introduction

During the bread making process, bromate is considered to be converted to bromide (Kurokawa et al., 1990), so that use of potassium bromate ($KBrO_3$) has been permitted as a flour improver for bread making in Japan and the USA in spite of its carcinogenicity (Kurokawa et al., 1986; DeAngelo et al., 1998). However, since ozonation of surface water for disinfection yields $KBrO_3$ as a by-product (Cavanagh et al., 1992), there is still concern regarding the human hazard presented by its renal carcinogenicity. As is clear from the specific use as a food additive, $KBrO_3$ is a potent oxidizing agent. This property is responsible for changes in DNA bases as well as lipid peroxidation (LPO), in the kidneys of treated rats (Chipman et al., 1998; Umemura et al., 1998). Since 8-hydroxydeoxyguanosine (8-OHdG), a form of guanine oxidized at C-8 position, is known to be fairly stable (Kasai and Nishimura, 1991), elevation of this oxidized base following $KBrO_3$ exposure implies involvement of oxidative stress in $KBrO_3$-induced carcinogenesis (Umemura and Kurokawa, 2006; Delker et al., 2006). Simultaneous treatment with antioxidants is known to prevent elevation of 8-OHdG and LPO induced by $KBrO_3$ (Cadenas and Barja, 1999; El-Sokkary, 2000), but it remains unclear how oxidative stress contributes to $KBrO_3$-carcinogenesis.

In two-stage model using *N*-ethyl-*N*-hydroxyethyl-nitrosamine as an initiator, $KBrO_3$ enhances renal tumorigenesis in both male and female rats (Kurokawa et al., 1985; Umemura et al., 1995). Also, short-term exposure to $KBrO_3$ in males was found to significantly elevate bromodeoxyuridine-labeling indices (BrdU-LIs) in proximal convoluted tubules (PCTs) in the same dose-dependent manner as evident in the promotion assay (Umemura et al., 1993). As a possible mode of action, we have proposed involvement of α_{2u}-globulin accumulation in $KBrO_3$-induced cell proliferation in males (Umemura et al., 2004). However, the fact that PCT BrdU-LIs in females exposed to $KBrO_3$ were also increased, albeit at higher doses than in males, implies the existence of other causal factors.

A two-stage model using nitrilotriacetate as a promoter has further shown that $KBrO_3$ possesses initiating activity for renal carcinogenesis in male rats (Umemura et al., 2006). In addition to previous positive results in several mutagenicity tests (Ishidate et al., 1984; Ishidate and Yoshioka, 1980; Hayashi et al., 1988), recent findings using isolated rat kidney cells (Nesslany et al., 2007) and

* Corresponding author. Tel.: +81 3 3700 9819.
E-mail address: umemura@nihs.go.jp (T. Umemura).

0300-483X/$ – see front matter © 2009 Published by Elsevier Ireland Ltd.
doi:10.1016/j.tox.2008.12.007

human peripheral lymphocytes (Kaya and Topaktas, 2007) point to genotoxic potential. Also, in an *in vivo* mutation assay using reporter gene transgenic rats, $KBrO_3$ proved capable of elevating the transgene mutation frequency (Umemura et al., 2006; Yamaguchi et al., 2008). Although induction of micronuclei in rat peripheral blood reticulocytes by $KBrO_3$ was inhibited by antioxidants (Sai et al., 1992), there have been few reports demonstrating clear relationships between oxidative stress and its genotoxicity.

Assessment of the participation of oxidative stress in $KBrO_3$ carcinogenesis is clearly necessary for accurate estimation of its hazard risk to humans. In the present study, taking advantage of the inhibitory effects of two different types of antioxidants, α-tocopherol (α-TP) and sodium ascorbic acid (SAA), changes in BrdU-LIs and α_{2u}-globulin accumulation in PCT, and transgene mutations in kidney DNA of male and female *gpt* delta rats given $KBrO_3$ were investigated.

2. Materials and methods

2.1. Chemicals

$KBrO_3$, α-TP and SAA were purchased from Wako Pure Chemical Industries (Osaka, Japan). Alkaline phosphatase was obtained from Sigma Chemical (St. Loius, MO, USA) and nuclease P1 was from Yamasa Shoyu (Chiba, Japan). Anti-BrdU monoclonal and anti-α_{2u}-globulin polyclonal antibodies were from DakoCytomation (Glostrup, Denmark) and R&D Systems, Ltd. (Minneapolis, MN, USA), respectively.

2.2. Animals, diet and housing conditions

The protocol for this study was approved by the Animal Care and Utilization Committee of the National Institute of Health Sciences. Five-week-old male and female *gpt* delta F344 rats carrying about five tandem copies of the transgene lambda EG10 per haploid genome were obtained from Japan SLC (Shizuoka, Japan). They were housed in polycarbonate cages (5 rats per cage) with hardwood chips for bedding in a conventional animal facility, maintained under conditions of controlled temperature (23 ± 2 °C), humidity (55 ± 5%), air change (12 times per hour), and lighting (12 h light/dark cycle) and were given free access to CRF-1 basal diet (BD; Charles River Japan) and tap water.

2.3. Animal treatments

Groups of 5 male and female *gpt* delta rats were administered $KBrO_3$ solution at a concentration of 500 ppm in the drinking water for 9 weeks. Additional subgroups of 5 male and female *gpt* delta rats were fed α-TP or SAA at a dose of 1% in the diet from 1 week prior to the $KBrO_3$ treatment until the end of the experiment. Further groups of 5 male and female rats each were given basal diet and distilled water (DW) throughout the experimental period as controls. All animals were injected with BrdU (100 mg/kg) i.p. twice a day for the final 2 days of the exposure and once on the day of termination, 2 h before killing. At the end of each period, the animals were killed under ethyl ether anesthesia and a part of left kidney was homogenized in Isogen (Nippon Gene, Tokyo, Japan) and stored at −80 °C until use for isolation of total RNA. The remaining left kidney was also stored at −80 °C for 8-OHdG measurement, Western blot analysis and *in vivo* mutation assays. Portions of right kidneys were fixed in ice-cold acetone for 3 days and processed for embedding in paraffin, sectioning (4 μm), and immunostaining for BrdU after histochemical demonstration of γ-glutamyltranspeptidase (γ-GT) activity. The remaining kidney tissue was fixed in buffered formalin and then routinely processed for embedding in paraffin, sectioning and immunostaining for α_{2u}-globulin.

2.4. Measurement of nuclear 8-OHdG

To prevent 8-OHdG formation as a byproduct during DNA isolation (Kasai, 2002), kidney DNA was extracted by a slight modification of the method of Nakae et al. (1995). Briefly, nuclear DNA was extracted with a commercially available DNA Extractor WB Kit (Wako Pure Chemical Industries, Ltd.) containing an antioxidant NaI solution to dissolve cellular components. For further prevention of autooxidation in the cell lysis step, deferoxamine mesylate (Sigma Chemical Co.) was added to the lysis buffer (Helbock et al., 1998). The DNA was digested to deoxynucleotides with nuclease P1 and alkaline phosphatase, and levels of 8-OHdG (8-OHdG/10^5 deoxyguanosine) were assessed by high-performance liquid chromatography (HPLC) with an electrochemical detection system (Coulochem II, ESA, Bedford, MA, USA).

2.5. Immunohistochemical procedures

For immunohistochemical staining of BrdU, sections were treated sequentially with normal horse serum, monoclonal mouse anti-BrdU (1:100), biotin-labeled horse anti-mouse IgG (1:400), and avidin-biotin-peroxidase complex (ABC) after denaturation of DNA with 4N HCl. Before the denaturation step, sections were processed histochemically for demonstration of γ-GT activity by the method of Rutenburg et al. (1969) using L-glutamyl-4-methoxy-β-naphtylamide (Polysciences Ltd., Warrington, PA, USA) as the substrate in order to assist in distinguishing the three kinds of tubules, as previously described (Umemura et al., 1992). The sites of peroxidase binding were demonstrated by incubation with 3,3′-diaminobenzidine tetrahydrochloride (Sigma Chemical Co.). For immunohistochemical staining of α_{2u}-globulin, sections were treated sequentially with normal goat serum, polyclonal rabbit anti-α_{2u}-globulin (1:100), biotin-labeled goat anti-rabbit IgG (1:400), and ABC after denaturation of DNA with 4N HCl. The immunostained sections were lightly counterstained with hematoxylin for microscopic examination.

2.6. Cell proliferation quantification

At least 3000 tubule cells in each kidney were counted and BrdU-LIs were calculated as the percentages of cells positive for BrdU incorporation.

2.7. Western blotting for α_{2u}-globulin

Kidney samples were homogenized with a Teflon homogenizer in ice-cold 50 mM Tris–HCl, pH 7.4 containing 0.25 M sucrose and a 1% protease inhibitor cocktail (Sigma Chemical Co.). The homogenate was centrifuged for 10 min at 10,000 × g, 4 °C, and the resulting supernatant was collected. Protein concentrations were determined with a BCA Protein Assay kit (Pierce Biotechnology Ltd., Rockford, IL, USA). The samples containing 20 μg protein were resolved by SDS-PAGE, transferred to Immobilon-P membranes (Millipore Corporation, Bedford, MA, USA) and analyzed with anti-α_{2u}-globulin (1:200), as well as anti-β-actin as a loading control (1:8000, Sigma Chemical Co.). Appropriate peroxidase-conjugated secondary antibodies (1:2000, Dako Cytomation) were used to detect proteins with ECL Plus (Amersham Bioscience Corp., Piscataway, NJ, USA) reagents.

2.8. In vivo mutation assays

6-TG and Spi^- selections were performed as previously described (Umemura et al., 2007) using the first three animals each group. Briefly, genomic DNA was extracted from the kidneys of the first 3 animals in each group, and lambda EG10 DNA (48 kb) was rescued as phages by *in vitro* packaging.

For 6-TG selection, packaged phages were incubated with *Escherichia coli* YG6020, which expresses Cre recombinase, and converted to plasmids carrying *gpt* and chloramphenicol acetyltransferase. Infected cells were mixed with molten soft agar and poured onto agar plates containing chloramphenicol and 6-TG. In order to determine the total number of rescued plasmids, 3000-fold diluted phages were used to infect YG6020, and poured on plates containing chloramphenicol without 6-TG. The plates were then incubated at 37 °C for selection of 6-TG-resistant colonies. Positively selected colonies were counted on day 3 and collected on day 4. The mutant frequency (MF) was calculated by dividing the number of *gpt* mutants by the number of rescued phages.

For Spi^- selection, packaged phages were incubated with *E. coli* XL-1 Blue MRA for survival titration and *E. coli* XL-1 Blue MRA P2 for mutant selection. Infected cells were mixed with molten lambda-trypticase agar plates. Next day, plaques (Spi^- candidates) were punched out with sterilized glass pipetters and the agar plugs were suspended in SM buffer. In order to confirm the Spi^- phenotype of candidates, the suspensions were spotted on three types of plates where XL-1 Blue MRA, XL-1 Blue MRA P2, or WL95 P2 strains were spread with soft agar. Real Spi^- mutants, which made clear plaques on every plate, were counted.

For characterizing the mutation spectra of *gpt* mutants, a 739 bp DNA fragment containing the 456 bp coding region of the *gpt* gene was amplified by PCR as described previously (Nohmi et al., 2000). DNA sequencing was performed with the Big Dye™ Terminater Cycle Sequencing Ready Reaction (Applied Biosystems, Foster City, CA, USA) on an ABI PRISM™ 310 Genetic Analayzer (Applied Biosystems).

3. Results

As shown in Fig. 1, 8-OHdG levels in kidney DNA of male and female *gpt* delta rats given $KBrO_3$ were significantly increased as compared to the controls. Although the levels in *gpt* delta rats of both sexes co-treated with α-TP or SAA were still significantly higher than the controls, significant decreases in either sex of rats were evident as compared to $KBrO_3$-treated animals.

PCT BrdU-LIs in male and female gpt delta rats exposed to $KBrO_3$, with or without antioxidants, are shown in Fig. 2. In the males, $KBrO_3$ exposure induced prominent rise of BrdU-LIs with statistical significance, which was not affected by α-TP or SAA treatment. In the females, $KBrO_3$ significantly increased BrdU-LIs as in the males,

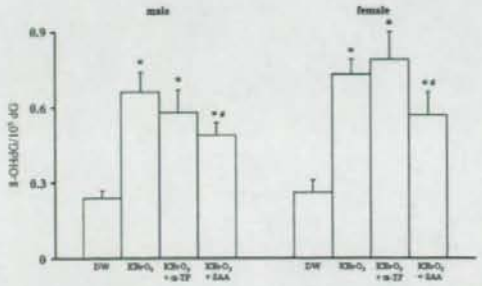

Fig. 1. 8-OHdG levels in kidneys of male and female *gpt* delta rats co-treated with $KBrO_3$ and α-TP or SAA. Values are means ± SDs of data for 5 rats. $^*p < 0.01$, significantly different from the controls (DW). $^\#p < 0.01$, significantly different from the $KBrO_3$ alone group.

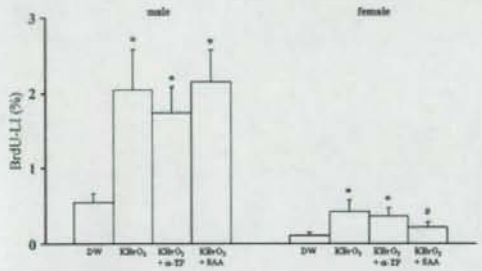

Fig. 2. BrdU-LIs for proximal convoluted tubules (PCT) of male and female *gpt* delta rats co-treated with $KBrO_3$ and α-TP or SAA. Values are means ± SDs of data for 5 rats. $^*p < 0.01$, significantly different from the controls (DW). $^\#p < 0.01$, significantly different from the $KBrO_3$ alone group.

but in this case, co-treatment with SAA, but not α-TP, was associated with suppression of the elevation.

Immunohistochemical data for α_{2u}-globulin are shown in Fig. 3(A–E). Because α_{2u}-globulin is a male rat-specific urinary protein, in controls scattered accumulation was limited to males (Fig. 3 A). $KBrO_3$ caused accumulation of the protein only in males (Fig. 3 B), which was not inhibited by any antioxidant treatments (Fig. 3 C and D), no binding being evident even in the $KBrO_3$-treated female rats (Fig. 3 E). These findings were directly in line with Western blot results for α_{2u}-globulin (Fig. 3 F).

Data for *gpt* MFs analyzed by 6-TG selection are summarized in Tables 1 and 2. In the males, although statistical analysis could not be performed because no *gpt* mutant colonies were detected in one control rat, MFs in all the treated groups showed a tendency for increase (Table 1). Likewise, in the females, elevation of MFs in all the treated groups were found, the increase in the $KBrO_3$ alone group being statistically significant (Table 2). To characterize *gpt* mutations DNA sequencing was performed (Table 3). Among the groups in which the MFs were significantly increased, there were no common types of mutations. GC:AT transitions in α-TP treated males, GC:TA and AT:TA transversions in SAA treated males and single base deletions in $KBrO_3$ alone treated females showed the highest mutation frequencies. As shown in Table 4, there were no changes in Spi^- MFs in males. In all the treated females, a tendency for elevation of Spi^- MFs was apparent, with statistical significance in the α-TP treatment case (Table 5). However, co-treatment with the antioxidants did not appear to exert any effects on MFs for the *gpt* gene in the kidneys of rats given $KBrO_3$.

4. Discussion

In the present study, increases of 8-OHdG levels in kidney DNA of male and female rats following $KBrO_3$ exposure were significantly suppressed by SAA, but not α-TP. Although precise mechanisms responsible for the differences in efficacy between the two antioxidants remain to be determined, it has been reported that dietary ascorbic acid is capable of accumulating more effectively in renal cortical tissue of rats than is the case with dietary α-TP (Craven et al., 1997). In consideration of the fact that $KBrO_3$ is efficiently reduced by GSH at brush borders on the luminal surfaces of PCT cells (Murata et al., 2001), eventually yielding oxidative stress (Ballmaier and Epe, 1995, 2006), it is plausible that an aqueous antioxidant would exert preventive effects. Previous study demonstrated that dietary vitamin E inhibited 8-OHdG levels in kidney DNA induced by $KBrO_3$ at higher dose (Cadenas and Barja, 1999). The incompatible results might involve differences in the nature of damage to DNA produced by low vs. high doses of $KBrO_3$. In the present study, simultaneous treatment with SAA was in fact able to attenuate oxidative damage caused by $KBrO_3$.

$KBrO_3$ at a concentration of 500 ppm has been reported to promote tumor development in the rat kidney of both sexes (Kurokawa et al., 1985; Umemura et al., 1995). Induction of cell proliferation, regarded as a contributing factor, was observed even at 30 ppm of $KBrO_3$ in males, in contrast to the lowest effective dose in females being 250 ppm (Umemura et al., 2004). Interestingly, α_{2u}-globulin accumulation in the kidneys of male rats also occurred in a

Table 1
Effects of antioxidants on *gpt* mutant frequencies in the kidneys of male *gpt* delta rats given $KBrO_3$.

Treatment		Animal no.	Cm^R colonies ($\times 10^5$)	6-TG^R and Cm^R colonies	Mutant frequency ($\times 10^{-5}$)	Mean ± SD
Water	Diet					
DW	BD	1	6.0	0[a]	0	
		2	9.3	1	0.11	0.12
		3	7.7	2	0.26	
$KBrO_3$	BD	6	9.2	3	0.33	
		7	98.8	2	0.20	0.43 ± 0.29
		8	6.6	5	0.76	
$KBrO_3$	α-TP	11	8.7	8	0.92	
		12	5.4	8	1.48	1.14 ± 0.30
		13	9.7	10	1.03	
$KBrO_3$	SAA	16	10.1	3	0.30	
		17	7.8	6	0.77	0.53 ± 0.24
		18	9.3	5	0.53	

DW: Distilled water, BD: basal diet.
[a] Two colonies were found on the plate, but neither harbored any *gpt* mutations.